Title
Dissecting the Mechanism of Arp2/3 Complex Activation by Actin Filament Binding and the Regulation and Function of JMY in Cells

Author
Firat, Elif Nur

Publication Date
2010

Peer reviewed|Thesis/dissertation

Dissecting the Mechanism of Arp2/3 Complex Activation by Actin Filament Binding and the Regulation and Function of JMY in Cells

By

Elif Nur Firat

A dissertation submitted in partial satisfaction of the

requirements for the degree of

Doctor of Philosophy

in

Molecular and Cell Biology

in the

Graduate Division

of the

University of California, Berkeley

Committee in charge:

Professor Matthew D. Welch, Chair
Professor David G. Drubin
Professor Rebecca Heald
Professor Daniel A. Fletcher

Fall 2010

Dissecting the Mechanism of Arp2/3 Complex Activation by Actin Filament Binding and the Regulation and Function of JMY in Cells

by

Elif Nur Firat

ABSTRACT

Dissecting the Mechanism of Arp2/3 Complex Activation by Actin Filament Binding and the Regulation and Function of JMY in Cells

by

Elif Nur Firat

Doctor of Philosophy in Molecular and Cell Biology

University of California, Berkeley

Professor Matthew D. Welch, Chair

The cellular functions of the actin cytoskeleton require precise regulation of the polymerization and organization of actin filaments. Actin nucleation is one of the key control points in this regulation and is accelerated by the action of actin nucleating proteins. Mammalian cells express a diverse set of actin nucleating proteins, each of which has a distinct molecular mechanism of action and mode of regulation.

One of the major actin nucleating proteins in cells it the Arp2/3 complex, which nucleates new filaments from the sides of existing ones to generate Y-branched actin networks. To investigate the mechanism of Arp2/3 complex activation by actin filament binding, we mutated amino acid residues within the predicted actin binding surfaces of the ARPC2 and ARPC4 subunits of the complex and examined the biochemical properties of mutant complexes. Using this approach, we defined sites on ARPC2 and ARPC4 that are required for high-affinity binding to actin filaments. Biochemical characterization of the actin binding mutants revealed that actin binding is crucial for actin nucleation and Y-branch stability.

The junction-mediating and regulatory protein (JMY) was recently discovered as a new actin nucleating protein that is unique among such proteins because it nucleates actin through both Arp2/3-complex-dependent and Arp2/3-complex-independent mechanisms. To investigate the mechanism of JMY regulation, we examined the activity of full-length JMY in actin assembly *in vitro* and in cells. We found that full-length recombinant JMY and the truncated WWWCA region have comparable actin nucleating and Arp2/3-complex-activating abilities *in vitro*. In contrast, the ability of full-length JMY to polymerize actin is somewhat inhibited in cells, suggesting autoinhibition and posttranslational modifications as potential mechanisms for JMY regulation. We also showed that JMY localizes primarily to the cytosol, in addition to its localization to the nucleus, and induces formation of actin filament clusters in cytosol consistent with its *in vitro* activity. Finally, we discovered a new function for JMY in neuritogenesis, as a negative regulator of neurite outgrowth.

DEDICATION

To my husband Tufan Karalar and my parents Nurgül and Ahmet Fırat, who always give me love and support.

TABLE OF CONTENTS

LIST OF FIGURES

LIST OF TABLES

ABBREVIATIONS

A: acidic region

Arp: actin related protein

ARPC: actin related protein complex

B: basic

C: connector, or central, or cofilin homology region

CC: coiled-coil region

(E)GFP: (enhanced) green fluorescent protein

F-actin: filamentous actin (actin polymer)

GBD: GTPase binding domain

JMY: Junction-mediating and regulatory protein

K_d: dissociation constant

LAP: localization and affinity purification

N: N-terminal domain

NPF: nucleation promoting factor

N-WASP: neuronal Wiskott-Aldrich Syndrome protein

P: polyproline region

PRD: proline-rich domain

PIP_2: phosphatidylinositol (bis)-phosphate

RNAi: RNA interference

SHD: Scar-homology domain

TBR: tubulin-binding domain

WAHD1: WASH homology domain 1

WASH: WASP and Scar homolog

WASP: Wiskott-Aldrich Syndrome protein

WAVE: WASP and verprolin homolog

WHAMM: WASP homolog associated with actin, membranes and microtubules

WH2/W: WASP homology 2 domain

WMD: WHAMM membrane interaction domain

WT: wild-type

ACKNOWLEDGEMENTS

First and foremost, I would like to thank my advisor Matt Welch. Matt was the most helpful and supportive advisor any student could hope for. With his supervision, support, patience, inspiration and constant encouragement, my six years of graduate life turned out to be a memorable learning and research experience, as well as a wonderful opportunity for professional development and self-transformation. He always made time to meet with me and encouraged further my work at every step. When I was most discouraged about what it seemed like the never ending failing experiments, he always showed me that there is light at the end of the tunnel. More than anyone else, Matt taught me to think big, communicate clearly, and challenge myself in science. He also taught me how to compartmentalize my life when I got married and when I had my son Mehmet. I couldn't have completed my dissertation without his support and guidance.

I also want to thank the members of my thesis committee, Rebecca Heald, David Drubin, and Daniel Fletcher, for their encouragement. Their advice and ideas over the years have helped me appreciate the importance of getting diverse perspectives, regular input, and constructive criticism on my research. I am also grateful to Philip Tucker and Jon Beckwith for giving me summer internship opportunities in their lab as an undergraduate student from Turkey and setting me the great first role models of how to be a great scientist.

I met many wonderful colleagues and friends along the way during graduate school, and want to thank them for their friendship and help, in particular to the members of the Welch lab. Everyone in the Welch lab especially Robert Jeng, Erin Goley, Stephane Bodin, Anosha Siripala, Ken Campellone, Alisa Serio, Cat Haglund, Taro Ohkawa, Erin Benanti, Steve Duleh, Peter Hsiue and Shawna Reed contributed to my work one way or another. My day-to-day interactions with them are one of the things I look forward to most when I come into the lab. Erin Goley and Stephane Bodin were the people I looked up to when I was a rotation student in the lab and they shared their wisdom and experience with me during the first years of graduate school. Ken Campellone also deserves a big thank you because he mentored me in my dissertation project, shared his extensive scientific expertise with me and showed me what discipline means. Anosha Siripala and Cat Haglund were wonderful baymates and our many conversations in between the experiments were always fun. I am also thankful to the members of the Heald and Weis labs past and present for advice at our regular trilab meetings and sharing reagents and equipment. I would also like to thank my friends for moral support and positive encouragement over the years, especially Phuang Gip, Benjamin Freedman and Yusra Dogan.

For more reasons than one, I could not have completed graduate school without the support of my loving family. It is difficult to express my appreciation to my mom, dad and sisters because it is so boundless. I have learned so much from my parents and I appreciate all of the sacrifices that they have made for me. I am grateful to them both for being wonderful role models to me and now, to my son Mehmet. My sisters, Melike and Mehpare, are my most enthusiastic cheerleaders and my best friends. Since my son Mehmet's birth, my family, in

particular my mom and mother-in-law, have been especially supportive, staying with us as we fumbled our way through the early days of parenthood.

I am deeply grateful for my husband, Tufan for his constant love and strength throughout the years. Without him, and his ability to raise my spirits when I was most discouraged, I could have never made it this far. Tufan is the only person who could have endured a three-hour commute everyday to his job in Sunnyvale (50 miles each way) so that I might spend less of my time commuting and more of my time doing research. I am also thankful to my son, Mehmet for being the best newborn at a critical time. Mehmet arrived towards the ends of my graduate work and has made my life ever so much more exciting and provided the most enjoyable type of distraction from dissertation woes. He is such a bundle of joy and laughter in our lives.

CHAPTER 1

New mechanisms and functions of actin nucleation

Note: The majority of information presented in this chapter was included in the publication:

Firat-Karalar, E.N. and Welch, M.D. (2010) "New mechanisms and functions of actin nucleation." Curr Opin Cell Biol.

Introduction

Actin is one of the most highly conserved and abundant proteins in eukaryotic cells and is a major constituent of the cytoskeleton. Actin monomers (G-actin) assemble to form polarized filaments (F-actin) that have a fast-growing barbed end and a slower-growing pointed end. The first step in the assembly of actin filaments is nucleation, which is defined as the formation of a stable multimer of actin monomers. This is the rate-limiting step in polymerization due to the instability of actin dimer intermediates and the activity of actin monomer-sequestering proteins that suppress spontaneous nucleation in cells. To overcome the kinetic hurdle for nucleation, cells use a diverse set of actin-nucleating proteins, including the actin-related protein 2/3 (Arp2/3) complex, formins and tandem-monomer-binding nucleators. These proteins play important roles in many essential cellular processes.

In this introductory chapter, I first compare the biochemical mechanisms of actin nucleation, focusing on recent advances and newly-discovered nucleators. I next describe progress in our understanding of the function of these nucleators in key actin-dependent processes including membrane trafficking, cell migration and division, examining how the characterization of known nucleators and the identification of new nucleators has revealed new ways in which actin polymerization contributes to cell function.

Actin nucleators and their mechanisms of action – old news and recent developments

The Arp2/3 complex

The first major actin nucleator to be discovered was the Arp2/3 complex, which is composed of evolutionarily-conserved subunits including the actin-related proteins Arp2 and Arp3 and five additional subunits ARPC1-5 (reviewed in (Goley and Welch, 2006)). The Arp2/3 complex by itself is an inefficient nucleator, and its activation requires binding to the sides of actin filaments and to proteins called nucleation promoting factors (NPFs) that have WCA domains consisting of G-actin binding WH2 (W) domains and Arp2/3-binding central/acidic (CA) sequences. Once activated, the Arp2/3 complex nucleates the formation of new filaments that extend from the sides of existing filaments at a 70° angle to form a Y-branched network (Fig. 1.1, left panel).

Although the ability of the Arp2/3 complex to nucleate Y-branched arrays is well-characterized, the mechanism of nucleation and branching is not fully understood. The most recent model of the Y-branch was obtained by docking the atomic-resolution crystal structure of an inactive conformation of the Arp2/3 complex into a 3D reconstruction of the branch obtained by electron tomography (Rouiller et al., 2008). This study suggested that Arp2 and Arp3 interact with the pointed end of the daughter filament while the remaining subunits, in particular ARPC2 and ARPC4, make substantial contacts with the mother filament. However, the functional importance of specific subunits and surfaces of the complex has only begun to be thoroughly investigated. Recent studies

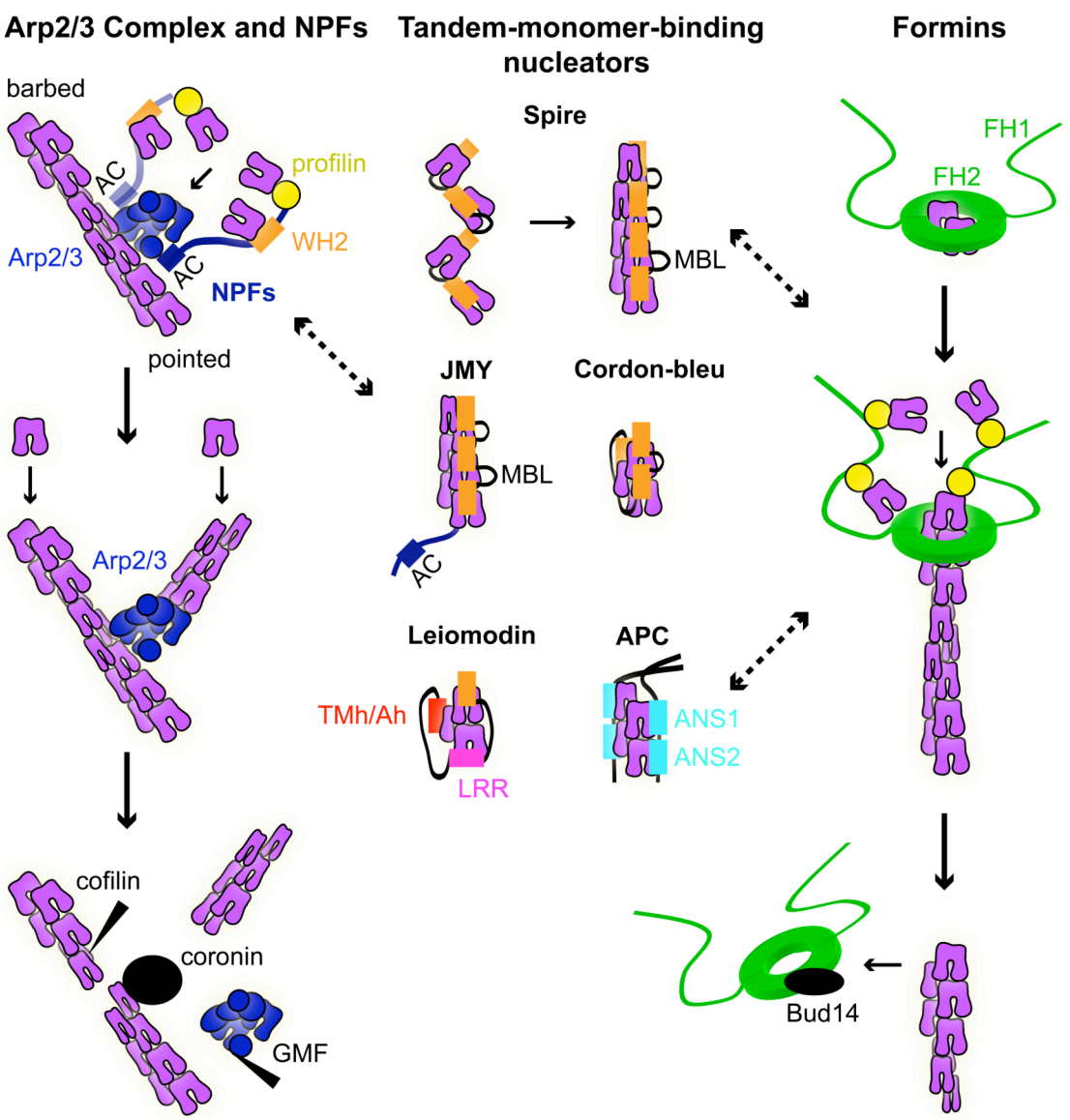

Figure 1.1: Models for actin nucleation

Left: Arp2/3 complex is activated by binding to the CA region of NPFs and to the side of actin filaments. In turn, NPFs bind actin monomers via their WH2 domains and profilin-actin monomers via their proline-rich regions, and deliver these to a nucleating complex. NPF dimerization enhances their activity, suggesting that dimers may bind to two sites on the Arp2/3 complex. After branch formation, cofilin and GMF stimulate debranching by binding to F-actin and Arp2/3 complex, respectively. Coronin binds both to F-actin and Arp2/3 complex, replaces Arp2/3 complex, and synergizes with cofilin to promote debranching. *Middle:* Tandem-monomer-binding nucleators bring together actin monomers through their clustered actin-binding motifs to form a nucleus. Spire and JMY stabilize actin monomers aligned along the long-pitch helix with their WH2 domains and monomer-binding linkers (MBL). Cordon-bleu, leiomodin

and dimeric APC, with their combination of WH2 domains, leucine rich repeats (LRR), tropomyosin and actin-binding helices (Tmh/Ah), and actin-nucleating sequences (ANS1-2), stabilize cross-filament interactions along the short-pitch helix of an actin filament. *Right:* Formins generate actin polymerization nuclei by stabilizing actin dimers through their homodimeric FH2 domains. The FH2 dimer stays processively attached to the barbed end of an actin filament as the flanking FH1 domains deliver profilin-actin to the barbed end for continued elongation. In yeast, Bud14p interacts with the FH2 domain and displaces formins from growing barbed ends. Dotted arrows point to the cross-talk between different actin nucleators.

employing mutagenesis of conserved surface residues on ARPC1, ARPC2 and ARPC4 have defined features that are functionally important for activity. In particular, residues on a conserved surface on ARPC2 and ARPC4 that is predicted to lie close to the mother filament in the Y-branch (Rouiller et al., 2008) were shown to be required for efficient actin nucleation, as well as for high affinity actin filament binding and Y-branch stability (Daugherty and Goode, 2008; Goley et al., 2010). Moreover, a conserved surface on ARPC1 was shown to be important for nucleation and binding to the WCA domain of the NPF Las17 (the *Saccharomyces cerevisiae* ortholog of the mammalian NPF WASP) (Balcer et al., 2010). Further mutational analyses combined with structural studies are needed to elucidate the detailed mechanism by which the Arp2/3 complex nucleates and branches filaments.

Because actin nucleation by the Arp2/3 complex requires the activity of NPFs, understanding NPF function and regulation is central to determining the mechanism of actin nucleation. Mammalian cells express several NPFs, including the well-characterized Wiskott-Aldrich Syndrome protein (WASP), neuronal WASP (N-WASP), three WASP and verprolin homologs (WAVEs), and the more recently identified WASP homolog associated with actin, membranes and microtubules (WHAMM), WASP and Scar homolog (WASH), and junction mediating regulatory (JMY) protein. The canonical mode of regulation of NPFs is via allosteric modulation of the accessibility of the WCA domain, either by autoinhibition through intramolecular interactions between the WCA and upstream domains of the NPF, as is the case for WASP and N-WASP (reviewed in (Derivery and Gautreau, 2010)), or trans-regulation by interacting proteins, as was shown for the WAVEs (Ismail et al., 2009; Lebensohn and Kirschner, 2009). Recent studies have also identified oligomerization as another layer of NPF regulation, based on the findings that dimerization of the WCA region increases the affinity of NPFs for the Arp2/3 complex and the efficiency of actin nucleation (Padrick et al., 2008). Thus, oligomerization can act together with allostery to enable NPFs to integrate a wide variety of cellular inputs that lead to activation of the Arp2/3 complex.

In addition to exploring the mechanisms of Arp2/3 complex activation, recent work has begun to elucidate the mechanisms of Arp2/3 complex inactivation and recycling through a process termed debranching. It has been known for some time that ATP hydrolysis by actin and the Arp2 subunit of the Arp2/3 complex (Goley and Welch, 2006), as well as binding of coronin (Cai et al., 2008), promote debranching and recycling of the Arp2/3 complex. More recent studies identified two new molecular players important for debranching: actin-depolymerizing factor (ADF)/cofilin and the ADF/cofilin superfamily protein glia maturation factor (GMF). These factors stimulate debranching through two distinct mechanisms (Fig. 1.1, left panel). ADF/cofilin, a filament severing protein, is proposed to stimulate debranching by directly competing with Arp2/3 for binding to F-actin as well as by causing a structural change in actin that reduces the affinity for Arp2/3 (Chan et al., 2009). These experiments were performed with ADF/cofilin purified from *Schizosaccharomyces pombe*, and it has not yet been reported whether one or more of the three ADF/cofilin family proteins expressed in mammalian cells (ADF, cofilin-1, and cofilin-2), which have

some differences in their biochemical activities (Bernstein and Bamburg, 2010), might also regulate debranching. In contrast to ADF/cofilin, GMF binds to the Arp2/3 complex but not to F-actin, and it prunes daughter filaments at branch points and inhibits Arp2/3-mediated nucleation of new filaments (Gandhi et al., 2010; Nakano et al., 2010). In the future, it will be important to address how the activities of Arp2/3-activating and Arp2/3-debranching proteins are coordinated to control Y-branch dynamics in cells.

Formins

The second major class of actin nucleators to be identified was the formins (reviewed in (Chesarone et al., 2010)). In contrast to the Arp2/3 complex, they are multidomain proteins that function as dimers to assemble unbranched actin filaments. Formins both nucleate actin and act as elongation factors that processively associate with growing barbed ends (Fig. 1.1, right panel), a phenomenon that has now been directly observed by tracking quantum dots coated with formins riding filament ends (Paul and Pollard, 2009). Processive association of formins with growing ends allows the addition of actin subunits while preventing capping proteins from terminating polymerization. The defining structural feature of formins is their conserved formin homology (FH) FH1 and FH2 domains. The homodimeric FH2 domain is thought to catalyze actin filament nucleation by stabilizing actin dimers (Fig. 1.1, right panel), although the FH2 domains of different formins vary widely in their nucleation activity. Elongation is then stimulated by the proline-rich FH1 domain, which binds to and increases the local concentration of profilin-bound G-actin to enable its delivery to the barbed end.

Recent work aimed at understanding the mechanism of action of formins has focused on the processive association with elongating filaments, and in particular the source of energy for this process. Nevertheless, the mechanism remains controversial. One study proposed that the energy for processive movement is derived from ATP hydrolysis on actin that is coupled to addition of profilin-actin onto barbed ends (Romero et al., 2007). However, a more recent study concluded that ATP hydrolysis on actin is not required for processivity, and instead postulated that the energy is derived from the binding of actin subunits to the barbed end (Paul and Pollard, 2009). Further investigation is required to resolve this controversy, and future efforts will focus on not only energetics but also on the structural basis for both nucleation and elongation, as well as potential mechanistic diversity within the formin family.

Apart from the mechanism of formin-mediated nucleation and elongation, recent studies have also characterized various modes of formin regulation. Formin activities can be regulated at multiple points, including initial activation, actin nucleation and elongation, and inactivation and recycling. The best understood mechanism of regulation is allosteric autoinhibition through intramolecular interactions between the Dia autoregulatory domain (DAD) and Dia inhibitory domain (DID) (Chesarone et al., 2010), similar to that discussed above for the NPFs WASP and N-WASP. Trans-regulation of formins by interacting proteins has since emerged as another mode of regulation. Previous

studies had identified two proteins that inhibit formin activity in vitro, Dia-interacting protein/WASP interacting SH3 protein (DIP/WISH) (Eisenmann et al., 2007) and Spire (Quinlan et al., 2007), although Spire is also thought to cooperate with formins to assemble actin filaments in *Drosophila melanogaster* oocytes (Dahlgaard et al., 2007). More recently, *S. cerevisiae* Bud14p was identified as an inhibitor of the formin Bnr1p. Bud14p was shown to displace Bnr1p from growing barbed ends, and to restrict the length of actin filaments elongated by formins in vitro and in cells (Chesarone et al., 2009). A second mechanism to attenuate formin-mediated elongation involves the actin-binding protein tropomyosin, which promotes annealing of actin filaments in a manner that can trap formins within the filament and promotes displacement of formins from barbed ends (Skau et al., 2009). These studies suggest that formin displacement may be a critical point of regulation, and future studies will need to address how allosteric activation and formin displacement are coordinated in the formin regulatory cycle.

Tandem-monomer-binding nucleators

The third group of actin nucleators includes Spire, cordon-bleu (Cobl), leiomodin (Lmod) (reviewed in (Qualmann and Kessels, 2009)) and the recently described JMY (Zuchero et al., 2009) and adenomatous polyposis coli (APC) (Okada et al., 2010). These contain tandem G-actin-binding motifs, which bring together monomers to form a polymerization nucleus. In addition to nucleating actin assembly, Spire has also been reported to sever actin filaments and modulate barbed end polymerization (Bosch et al., 2007). While the WH2 domain is the most common actin-binding motif in these nucleators, they also have additional actin-binding elements. These include the monomer-binding linker (MBL) in Spire and JMY, tropomyosin and actin-binding helices (Tmh/Ah) and the leucine-rich repeat (LRR) in leiomodin, and the actin-nucleating sequences (ANS1, 2) in APC. This heterogeneity implies that nucleators with distinct domain architecture may remain to be identified.

Despite their shared ability to nucleate actin by gathering monomers into a nucleation complex, members of this family have been proposed to form nuclei with distinct structural arrangements (Fig. 1.1, middle panel). For example, Spire and JMY (Zuchero et al., 2009) have been proposed to stabilize monomers aligned along the long-pitch helix of the filament, whereas Cobl, Lmod (Qualmann and Kessels, 2009) and APC (Okada et al., 2010) have been proposed to stabilize cross-filament interactions along the short-pitch helix. However, little structural information is available to verify these proposed mechanisms. An initial X-ray scattering analysis of a Spire-like hybrid WH2 cluster suggested that the nucleus consisted of actin subunits aligned along the long-pitch helix of the filament (Rebowski et al., 2008). However, a more recent determination of the structure of a Spire-actin nucleus by X-ray crystallography suggested that actin monomers are initially organized in a compacted conformation that isomerizes to form a straight long-pitch configuration upon addition of monomers in cross-filament interactions (Ducka et al., 2010). The configuration of the APC-actin nucleus may be distinct, as APC differs from other members of this class in that its minimum nucleating domain has been shown to form a dimer in vitro (Okada

et al., 2010). Further structural and biochemical studies are needed to define the configuration of the actin nucleus and the mechanism of actin assembly by members of this class of nucleators.

Cooperation between different families of nucleators

Emerging evidence suggests that these nucleator families do not necessarily function individually, and that cross-talk occurs between different nucleators in cells. For example, Spire directly interacts with the formin Cappuccino (Capu) in vitro, and this interaction blocks Capu actin nucleation activity while enhancing Spire activity (Quinlan et al., 2007). Spire and Capu also function together to organize a dynamic network of actin filaments in *Drosophila* oocytes (Dahlgaard et al., 2007). APC synergizes with the formin mammalian homolog of Diaphanous 1 (mDia1) to promote actin nucleation in vitro and ectopic actin assembly in cells (Okada et al., 2010). JMY both nucleates actin itself and cooperates with the Arp2/3 complex to nucleate actin in vitro, although how these activities are coordinated in cells is not known (Zuchero et al., 2009). Finally, the NPF WASH was shown to function together with Spire and the formin Capu to regulate actin and microtubule organization during *Drosophila* oogenesis (Liu et al., 2009b). These findings suggest that an intricate interplay between different actin nucleators may enable increased spatial and temporal control over actin assembly in cells and allow greater flexibility in the overall architecture of actin filament networks.

Cellular functions of actin nucleators

The different classes of actin nucleators discussed above play important roles in a variety of cellular processes. Here, we focus on recent advances and controversies related to the function of actin nucleators in three key actin-dependent processes: membrane trafficking, leading edge protrusion during cell migration, and cell division.

Membrane trafficking

Actin polymerization plays a role in many membrane trafficking events including endocytic internalization, endocytic transport, and endoplasmic reticulum (ER)-to-Golgi transport. One function of actin nucleation common to each of these processes is the dynamic shaping and remodeling of membranes. The actin nucleators that contribute to these processes span all three classes and include the Arp2/3 complex and its NPFs, the inverted formin 2 (INF2), and the tandem-monomer-binding nucleator Spire.

The functional importance of actin polymerization in the internalization step of clathrin-mediated endocytosis is well established and many of the molecular players have been identified, particularly in the yeast *S. cerevisiae*, where the process is intensively studied (reviewed in (Robertson et al., 2009)).

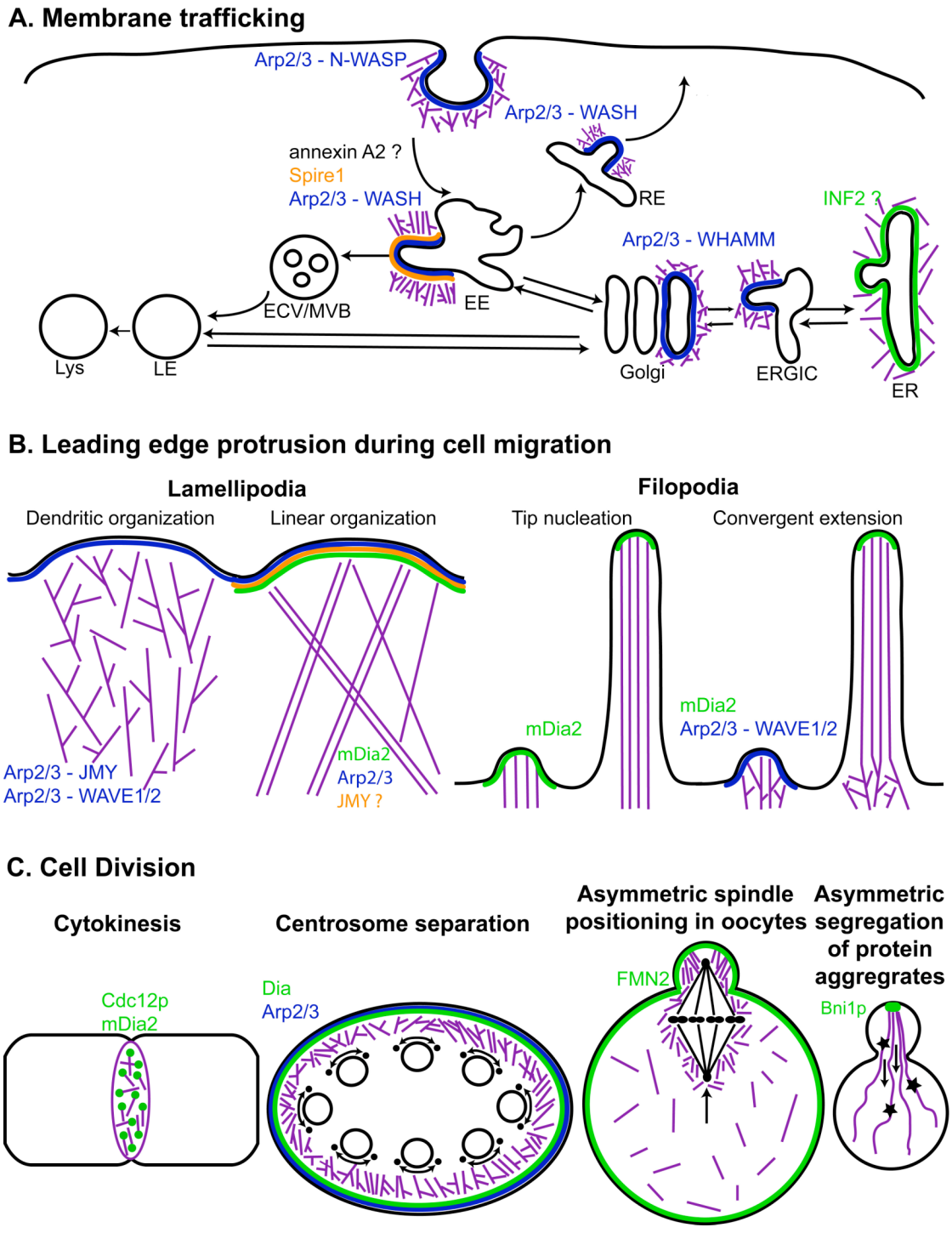

Figure 1.2: Models of the cellular localization and function of actin nucleators

(A) A depiction of the role of actin nucleators in membrane-trafficking events including endocytic internalization as well as various stages of endocytic and ER-to-Golgi trafficking. Abbreviations: EE, early endosomes; ECV/MVB, endosomal carrier vesicles/multivesicular bodies; LE, late endosomes; RE, recycling

endosomes; Lys, lysosome; ER, Endoplasmic reticulum; ERGIC, endoplasmic reticulum-Golgi intermediate compartment. (B) Diagram of the role of actin nucleators in lamellipodia and filopodia. In the dendritic organization model of actin organization in lamellipodia, branched actin networks are nucleated by the Arp2/3 complex and the NPFs WAVE1/2 and JMY. In the linear organization model, filaments are nucleated by the Arp2/3 complex but are unbranched, or are nucleated by mDia2 or perhaps JMY. In the tip nucleation model of filopodium formation, bundled arrays of actin filaments are nucleated by mDia2, whereas in the convergent elongation model, filaments are nucleated by the Arp2/3 complex and WAVE1/2, and are elongated by mDia2. (C) Cartoons depicting the role of actin nucleators in cell division. During cytokinesis, formins (Cdc12p in yeast, mDia2 in mammalian cells) nucleate actin filaments from multiple nodes at the division site that then coalesce into the contractile ring in the search, capture, pull and release model. During centrosome separation, dynamic actin reorganization by Dia and Arp2/3 drives centrosome separation in the early syncytial *Drosophila* embryo. For asymmetric spindle positioning in mouse oocytes, FMN2 nucleates a dynamic actin network that moves the spindle to the cell cortex. During the segregation of protein aggregates in *S. cerevisiae*, Bni1p generates actin cables extending from the polarisome that are required for transport of protein aggregates from the daughter to the mother cell. In (A), (B), and (C) nucleators are color-coded as follows: Arp2/3 complex and NPFs (blue), formins (green), tandem-monomer-binding nucleators (yellow). Question marks indicate that the precise role of the nucleating protein is unclear.

The Arp2/3 complex is the primary actin nucleator during this process, and it is activated by a number of different NPFs including Las17p/WASp, Abp1p, Pan1p, Myo3p and Myo5p in *S. cerevisiae,* and N-WASP in mammalian cells. Despite the fact that many key molecules have been identified, the biochemical and biophysical contributions of actin polymerization are a matter of active investigation. Our relatively detailed understanding of both the molecules and subprocesses involved in endocytic internalization has enabled the recent development of a theoretical model that describes how membrane shaping is coupled with the underlying biochemical reactions (Liu et al., 2009a). According to this model, actin nucleation and polymerization is important for the generation of an initial force that drives the shaping of membrane invaginations, resulting in the initiation of a positive feedback loop involving the recruitment of Bin/Amphiphysin/Rvs (BAR) domain proteins and lipid phosphatases, and the development of $PI(4,5)P_2$ lipid phase segregation. This phase separation is thought to generate an interfacial force that constricts the membrane invagination and drives vesicle scission. Interestingly, actin polymerization by the Arp2/3 complex and activated N-WASP in the absence of other factors was recently shown to drive vesicle scission from tubulated membrane intermediates in a reconstituted system in vitro (Romer et al., 2010). These studies support the emerging view that actin nucleation and polymerization induce membrane deformation and scission via a capacity to generate force and/or promote lipid phase segregation.

In contrast to the case of endocytic internalization, the role of actin in later stages of endocytic trafficking is poorly understood and the molecular players are just now being identified (Fig. 1.2A). A handful of nucleating proteins that function in early-to-late endosome transport have been identified, including the NPF WASH as well as Spire1 and annexin A2. WASH localizes to patches on early and recycling endosomes, where it promotes Arp2/3 complex-induced actin nucleation (Derivery et al., 2009; Duleh and Welch, 2010; Gomez and Billadeau, 2009). WASH has been implicated in modulating endosome shape and is hypothesized to function in receptor recycling, retromer-mediated endosome-to-Golgi transport, and endosome-to-lysosome trafficking. Although native WASH was recently shown to exist in a multiprotein complex, how the activity of the complex is regulated has not yet been determined (Derivery et al., 2009; Gomez and Billadeau, 2009; Jia et al., 2010). In addition to WASH and the Arp2/3 complex, Spire1 has also been localized to early endosomes and shown to bind to and function with annexin A2 in nucleating F-actin patches (Morel et al., 2009). Although these studies highlight the functional importance of actin nucleation in shaping the membranes of early endosomes and in enabling endosomal trafficking, the precise mechanistic contribution of actin remains unknown. Because actin-mediated membrane reorganization facilitates vesicle scission during internalization, it is tempting to speculate that actin polymerization might perform a similar function during later stages of endocytic trafficking.

In addition to playing a role in endocytosis, actin nucleation has also been implicated in ER-to-Golgi transport (Fig. 1.2A). The NPF WHAMM localizes to the cis-Golgi apparatus, and functions in maintaining Golgi shape and facilitating ER-to-Golgi transport (Campellone et al., 2008). In addition,

WHAMM localizes to tubulo-vesicular membrane transport intermediates and promotes membrane tubulation and tubule elongation by inducing Arp2/3-mediated actin assembly and interacting with microtubules. Although WHAMM-mediated Arp2/3 activation remains the best-characterized way of nucleating actin during ER-to-Golgi transport, another nucleator was also recently implicated in this process. The formin INF2 was localized to the ER and was implicated in actin assembly in cells based on the observation that an activated mutant caused actin assembly and ER collapse onto the nucleus (Chhabra et al., 2009). Interestingly, INF2 was also implicated in basolateral-to-apical transcytosis in polarized hepatoma cells (Madrid et al., 2010). Future studies will address the role of actin nucleation in membrane trafficking by exploring more precisely the stages of transport that require actin, whether the role of actin is general or restricted to certain cargos, and what biophysical role actin nucleation plays in reshaping and remodeling membranes.

Leading edge protrusion during cell migration

In migrating cells, actin polymerization in flat membrane protrusions called lamellipodia and finger-like protrusions called filopodia provides the driving force for leading edge protrusion (reviewed in (Le Clainche and Carlier, 2008)). Widely-accepted models have proposed that lamellipodia are composed of Y-branched filament networks nucleated by Arp2/3 complex while filopodia are composed of linear bundles nucleated by formins. However, recent work has challenged some of these assumptions. These studies suggest that the molecular mechanisms of actin nucleation in lamellipodia and filopodia are likely to be complicated and involve cross-participation of diverse actin nucleators.

The dendritic nucleation model, which posits that the Arp2/3 complex and NPFs polymerize Y-branched filament networks, has long been the accepted model for actin nucleation in lamellipodia (Fig. 1.2B) (Le Clainche and Carlier, 2008). Evidence supporting this model comes from the observations that Y-branching is integral to Arp2/3 complex activity in vitro, that Arp2/3 is required for lamellipodium formation in cells, and that Y-branches were observed in lamellipodia by electron microscopy with Arp2/3 localized to branch points (Goley and Welch, 2006; Le Clainche and Carlier, 2008). However, this model has been challenged by a recent study in which actin filament networks in lamellipodia of live vitreously frozen cells were visualized by electron tomography (Urban et al., 2010). Using this method, individual filaments could be traced along the lamellipodium and were observed to be long and organized into doublets of X-links, but few Y-branches were seen (Fig. 1.2B). This finding opens a new debate about the dendritic nucleation model, and suggests an alternative model that does not rule out the importance of Arp2/3 complex for actin nucleation, but implies that Arp2/3 may not always form Y-branches in cells. Given the strength of the evidence supporting the dendritic nucleation model, discarding this model is premature, and additional confirmatory work is needed to buttress the case that Y-branches are indeed absent from actin networks within lamellipodia and other structures known to be assembled by the Arp2/3 complex.

Activation of the Arp2/3 complex in lamellipodia is known to be mediated by the WAVE subfamily of NPFs (Le Clainche and Carlier, 2008). More recently, the multifunctional actin nucleator JMY was also shown to localize to lamellipodia in migrating cells, and its depletion slowed migration while its overexpression enhanced migration (Zuchero et al., 2009). JMY was originally discovered as a transcriptional coactivator, and its function in cell migration was recently postulated to be due in part to a role in controlling cadherin expression and cell adhesion (Coutts et al., 2009). Moreover, the nucleating and Arp2/3-activating activities of JMY both appear to be important for its function in enhancing cell migration (Coutts et al., 2009; Zuchero et al., 2009). The dual ability of JMY to directly nucleate unbranched actin filaments and activate the Arp2/3 complex to polymerize branched actin filaments might help explain the presence of both filament populations in lamellipodia. The presence of a substantial population of unbranched filaments in lamellipodia also suggests the possible involvement of formins. However, evidence addressing a possible role for formins is only beginning to emerge. A melanoma-derived cell line was shown to require mDia2 for lamellipodium formation (Yang et al., 2007), although mDia2 was not required for membrane ruffling in HeLa cells (Beli et al., 2008). T cells (Sakata et al., 2007) and neutrophils (Shi et al., 2009) from mDia1 knockout mice exhibited impaired polarization and chemotaxis, further supporting the functional importance of formins during cell migration. Future experimental studies are required to determine how different actin nucleators work together to polymerize actin in lamellipodia and similar protrusive structures.

In filopodia, which contain bundled arrays of actin filaments, the precise role of actin nucleators is also a matter of active investigation and debate, and two competing models have been proposed. According to the tip nucleation model, filopodia arise by formin-mediated nucleation and elongation of linear filaments at the extending filopodial tip (Fig. 1.2B) (reviewed in (Mellor, 2010)). In support of this model, depletion of mDia2 in cells inhibits filopodium formation while overexpression of a constitutively active mutant induces it (Block et al., 2008; Hotulainen et al., 2009; Yang et al., 2007). Although a role for mDia2 is clear, whether it functions primarily to nucleate or to elongate existing filaments remains uncertain. The alternative model, termed convergent elongation, proposes that the bundle of filaments in filopodia originates from a branched network of filaments nucleated by Arp2/3 complex in lamellipodia (Fig. 1.2B). Initial support for this model came from electron micrographs showing that filaments in filopodia are continuous with those in lamellipodia (Svitkina et al., 2003), and from the observation that inhibition of Arp2/3 complex activity suppressed filopodium formation in neurons (Korobova and Svitkina, 2008). However, others have found that silencing of the Arp2/3 complex in melanoma cells does not abolish filopodium formation, suggesting that the requirement for the Arp2/3 complex may be cell-type dependent (Steffen et al., 2006). To further complicate matters, it was recently shown that the Arp2/3 complex localizes to puncta within filopodia of spreading cells that may correspond to lamellipodia activity within filopodia (Johnston et al., 2008), and to the heads of neuronal dendritic spines at the tips of dendritic filopodia (Hotulainen et al., 2009; Korobova and Svitkina, 2010). Continued examination of

the relationship between filopodia and lamellipodia, both at an ultrastructural and mechanistic level, is required to determine in what contexts actin nucleation in both structures is interdependent or separable.

Cell division

Actin nucleation also plays crucial and varied roles at several stages of cell division. The best-studied of these is the assembly of the contractile ring, which is essential for cytokinesis. Recent work has highlighted unexpected roles for actin in other facets of cell division, including centrosome separation and asymmetric positioning of the spindle and chromosomes in oocytes, as well as segregation of protein aggregates in yeast.

The molecular requirements for contractile ring assembly have been best characterized in the fission yeast *Schizosaccharomyces pombe*. The key actin nucleator in this system is the formin Cdc12p, which is essential for actin assembly in the contractile ring (reviewed in (Pollard, 2010)). How actin nucleation and elongation by Cdc12p contributes to contractile ring assembly is under active investigation. Cdc12p expressed by its native promoter localizes to a broad band of multiple nodes at the division site (Coffman et al., 2009). Actin filaments are nucleated from these nodes and elongate in random directions (Fig. 1.2C). Following actin filament nucleation, myosin-II activity is required for the nodes to coalesce into the contractile ring. Mathematical simulations of this process support a search, capture, pull and release model in which actin filaments nucleated by Cdc12p are transiently captured by myosin-II in neighboring nodes, which then pull nodes together (Vavylonis et al., 2008). Interestingly, ectopic expression of an activated mutant of Cdc12p results in contractile ring assembly in interphase, a process that requires not only actin assembly but also activation of other contractile ring factors, suggesting that Cdc12p may function as a regulator that drives ring assembly via multiple pathways (Yonetani and Chang, 2010). Studies in animal cells also provide evidence for the functional importance of formins during contractile ring assembly (Pollard, 2010). Most recently, the mammalian formin mDia2 was shown to localize to the cleavage furrow and perform important functions in actin assembly and cytokinesis (Watanabe et al., 2008; Watanabe et al., 2010). It remains to be seen whether formins in mammalian cells participate in contractile ring assembly via a mechanism similar to that seen in *S. pombe*, or by another pathway.

In addition having a role in contractile ring assembly, actin nucleation is important for other facets of cell division, including centrosome separation, spindle and chromosome movements, and segregation of damaged proteins (Fig. 1.2C). During cell divisions in the early syncytial *Drosophila melanogaster* embryo, centrosome separation is driven in part by microtubules and the motor dynein. However, this process was also recently shown to require actin nucleation by the Arp2/3 complex and the formin Diaphanous (Dia) (Cao et al., 2010). Centrosome separation in mammalian cells also depends in part on cortical actin and myosin (Rosenblatt et al., 2004), although a function for actin nucleators has not been investigated. Apart from its roles early in cell division, actin nucleation is also

important later, particularly in mammalian oocytes during female asymmetric meiotic divisions. Asymmetric divisions involve off-center positioning of the spindle and chromosomes, a process that in mouse oocytes depends on a dynamic actin network but not on microtubules. Actin nucleation by formin 2 (FMN2) was shown to play a key role in spindle and chromosome movement during this process (Azoury et al., 2008; Li et al., 2008; Schuh and Ellenberg, 2008). Whether the force for movement is derived from actin polymerization (Li et al., 2008) or myosin activity (Schuh and Ellenberg, 2008) is a matter of debate, although both force-generating mechanisms could operate at different stages of the process. A third facet of cell division that requires actin nucleation is the establishment of cellular age asymmetry in *S. cerevisiae*. In dividing yeast cells subjected to heat stress, aggregated proteins are segregated from daughter cells to mother cells, a process that is proposed to be related to aging of the mother cell (Liu et al., 2010). The formin Bni1p generates actin cables extending from the polarisome at the distal end of the daughter that are required for directional transport of protein aggregates to the mother cell. It is unclear whether actin polymerization itself drives transport or whether myosin motors also participate. Another formin, Bnr1p, also contributes to asymmetry by allowing protein aggregates in mother cells to merge into an inclusion body. It is an open question as to whether there is a similar protein quality control mechanism during division in other species. The involvement of actin nucleators in such a diverse array of processes is remarkable, and suggests that we are just scratching the surface in terms of our mechanistic understanding of the roles that these proteins play in cell division.

Conclusions

The past two years have seen key advances both in understanding the function of previously-recognized actin nucleators, and in identifying new ones. These advances have come from a combination of biochemical and structural studies aimed at deciphering the mechanisms of actin nucleation, and cell biological studies aimed at defining the functions of actin nucleators at a cellular and organismal level. However, many unanswered questions remain. For example, we know little about the structures of actin nucleators in their activated states, and advances in this area will be essential for understanding the mechanisms of nucleation in greater detail. Moreover, how upstream signal transduction pathways regulate the activity of nucleators needs to be determined at a biochemical level, especially for those that were only recently discovered. More detailed cell biological experiments are also required to explain the function and regulation of actin nucleation during distinct cellular processes. Lastly, emerging evidence has suggested that actin nucleators cooperate with and antagonize each other in vivo, overturning simplified models that assigned one nucleator to one cellular process. Systems-level approaches will be required to determine how the complex cast of molecular players and their interactions are integrated during cell function and behavior. Thus, future studies will allow us to better appreciate the complexity of cellular actin nucleation pathways.

References

Azoury, J., Lee, K.W., Georget, V., Rassinier, P., Leader, B., and Verlhac, M.H. (2008). Spindle positioning in mouse oocytes relies on a dynamic meshwork of actin filaments. Curr Biol *18*, 1514-1519.

Balcer, H.I., Daugherty-Clarke, K., and Goode, B.L. (2010). The p40/ARPC1 subunit of Arp2/3 complex performs multiple essential roles in WASp-regulated actin nucleation. J Biol Chem *285*, 8481-8491.

Beli, P., Mascheroni, D., Xu, D., and Innocenti, M. (2008). WAVE and Arp2/3 jointly inhibit filopodium formation by entering into a complex with mDia2. Nat Cell Biol *10*, 849-857.

Bernstein, B.W., and Bamburg, J.R. (2010). ADF/cofilin: a functional node in cell biology. Trends Cell Biol *20*, 187-195.

Block, J., Stradal, T.E., Hanisch, J., Geffers, R., Kostler, S.A., Urban, E., Small, J.V., Rottner, K., and Faix, J. (2008). Filopodia formation induced by active mDia2/Drf3. J Microsc *231*, 506-517.

Bosch, M., Le, K.H., Bugyi, B., Correia, J.J., Renault, L., and Carlier, M.F. (2007). Analysis of the function of Spire in actin assembly and its synergy with formin and profilin. Mol Cell *28*, 555-568.

Cai, L., Makhov, A.M., Schafer, D.A., and Bear, J.E. (2008). Coronin 1B antagonizes cortactin and remodels Arp2/3-containing actin branches in lamellipodia. Cell *134*, 828-842.

Campellone, K.G., Webb, N.J., Znameroski, E.A., and Welch, M.D. (2008). WHAMM is an Arp2/3 complex activator that binds microtubules and functions in ER to Golgi transport. Cell *134*, 148-161.

Cao, J., Crest, J., Fasulo, B., and Sullivan, W. (2010). Cortical Actin Dynamics Facilitate Early-Stage Centrosome Separation. Curr Biol.

Chan, C., Beltzner, C.C., and Pollard, T.D. (2009). Cofilin dissociates Arp2/3 complex and branches from actin filaments. Curr Biol *19*, 537-545.

Chesarone, M., Gould, C.J., Moseley, J.B., and Goode, B.L. (2009). Displacement of formins from growing barbed ends by bud14 is critical for actin cable architecture and function. Dev Cell *16*, 292-302.

Chesarone, M.A., DuPage, A.G., and Goode, B.L. (2010). Unleashing formins to remodel the actin and microtubule cytoskeletons. Nat Rev Mol Cell Biol *11*, 62-74.

Chhabra, E.S., Ramabhadran, V., Gerber, S.A., and Higgs, H.N. (2009). INF2 is an endoplasmic reticulum-associated formin protein. J Cell Sci *122*, 1430-1440.

Coffman, V.C., Nile, A.H., Lee, I.J., Liu, H., and Wu, J.Q. (2009). Roles of formin nodes and myosin motor activity in Mid1p-dependent contractile-ring assembly during fission yeast cytokinesis. Mol Biol Cell *20*, 5195-5210.

Coutts, A.S., Weston, L., and La Thangue, N.B. (2009). A transcription co-factor integrates cell adhesion and motility with the p53 response. Proc Natl Acad Sci U S A *106*, 19872-19877.

Dahlgaard, K., Raposo, A.A., Niccoli, T., and St Johnston, D. (2007). Capu and Spire assemble a cytoplasmic actin mesh that maintains microtubule organization in the Drosophila oocyte. Dev Cell *13*, 539-553

Daugherty, K.M., and Goode, B.L. (2008). Functional surfaces on the p35/ARPC2 subunit of Arp2/3 complex required for cell growth, actin nucleation, and endocytosis. J Biol Chem *283*, 16950-16959.

Derivery, E., and Gautreau, A. (2010). Generation of branched actin networks: assembly and regulation of the N-WASP and WAVE molecular machines. Bioessays *32*, 119-131.

Derivery, E., Sousa, C., Gautier, J.J., Lombard, B., Loew, D., and Gautreau, A. (2009). The Arp2/3 activator WASH controls the fission of endosomes through a large multiprotein complex. Dev Cell *17*, 712-723.

Ducka, A.M., Joel, P., Popowicz, G.M., Trybus, K.M., Schleicher, M., Noegel, A.A., Huber, R., Holak, T.A., and Sitar, T. (2010). Structures of actin-bound Wiskott-Aldrich syndrome protein homology 2 (WH2) domains of Spire and the implication for filament nucleation. Proc Natl Acad Sci U S A.

Duleh, S.N., and Welch, M.D. (2010). WASH and the Arp2/3 complex regulate endosome shape and trafficking. Cytoskeleton (Hoboken) *67*, 193-206.

Eisenmann, K.M., Harris, E.S., Kitchen, S.M., Holman, H.A., Higgs, H.N., and Alberts, A.S. (2007). Dia-interacting protein modulates formin-mediated actin assembly at the cell cortex. Curr Biol *17*, 579-591.

Gandhi, M., Smith, B.A., Bovellan, M., Paavilainen, V., Daugherty-Clarke, K., Gelles, J., Lappalainen, P., and Goode, B.L. (2010). GMF is a cofilin homolog that binds Arp2/3 complex to stimulate filament debranching and inhibit actin nucleation. Curr Biol *20*, 861-867.

Goley, E.D., Rammohan, A., Znameroski, E.A., Firat-Karalar, E.N., Sept, D., and Welch, M.D. (2010). An actin-filament-binding interface on the Arp2/3 complex is critical for nucleation and branch stability. Proc Natl Acad Sci U S A *107*, 8159-8164.

Goley, E.D., and Welch, M.D. (2006). The ARP2/3 complex: an actin nucleator comes of age. Nat Rev Mol Cell Biol *7*, 713-726.

Gomez, T.S., and Billadeau, D.D. (2009). A FAM21-containing WASH complex regulates retromer-dependent sorting. Dev Cell *17*, 699-711.

Hotulainen, P., Llano, O., Smirnov, S., Tanhuanpaa, K., Faix, J., Rivera, C., and Lappalainen, P. (2009). Defining mechanisms of actin polymerization and depolymerization during dendritic spine morphogenesis. J Cell Biol *185*, 323-339.

Ismail, A.M., Padrick, S.B., Chen, B., Umetani, J., and Rosen, M.K. (2009). The WAVE regulatory complex is inhibited. Nat Struct Mol Biol *16*, 561-563.

Jia, D., Gomez, T.S., Metlagel, Z., Umetani, J., Otwinowski, Z., Rosen, M.K., and Billadeau, D.D. (2010). WASH and WAVE actin regulators of the Wiskott-Aldrich syndrome protein (WASP) family are controlled by analogous structurally related complexes. Proc Natl Acad Sci U S A *107*, 10442-10447.

Johnston, S.A., Bramble, J.P., Yeung, C.L., Mendes, P.M., and Machesky, L.M. (2008). Arp2/3 complex activity in filopodia of spreading cells. BMC Cell Biol *9*, 65.

Korobova, F., and Svitkina, T. (2008). Arp2/3 complex is important for filopodia formation, growth cone motility, and neuritogenesis in neuronal cells. Mol Biol Cell *19*, 1561-1574.

Korobova, F., and Svitkina, T. (2010). Molecular architecture of synaptic actin cytoskeleton in hippocampal neurons reveals a mechanism of dendritic spine morphogenesis. Mol Biol Cell *21*, 165-176.

Le Clainche, C., and Carlier, M.F. (2008). Regulation of actin assembly associated with protrusion and adhesion in cell migration. Physiol Rev *88*, 489-513.

Lebensohn, A.M., and Kirschner, M.W. (2009). Activation of the WAVE complex by coincident signals controls actin assembly. Mol Cell *36*, 512-524.

Li, H., Guo, F., Rubinstein, B., and Li, R. (2008). Actin-driven chromosomal motility leads to symmetry breaking in mammalian meiotic oocytes. Nat Cell Biol *10*, 1301-1308.

Liu, B., Larsson, L., Caballero, A., Hao, X., Oling, D., Grantham, J., and Nystrom, T. (2010). The polarisome is required for segregation and retrograde transport of protein aggregates. Cell *140*, 257-267.

Liu, J., Sun, Y., Drubin, D.G., and Oster, G.F. (2009a). The mechanochemistry of endocytosis. PLoS Biol *7*, e1000204.

Liu, R., Abreu-Blanco, M.T., Barry, K.C., Linardopoulou, E.V., Osborn, G.E., and Parkhurst, S.M. (2009b). Wash functions downstream of Rho and links linear and branched actin nucleation factors. Development *136*, 2849-2860.

Madrid, R., Aranda, J.F., Rodriguez-Fraticelli, A.E., Ventimiglia, L., Andres-Delgado, L., Shehata, M., Fanayan, S., Shahheydari, H., Gomez, S., Jimenez, A., *et al.* (2010). The formin INF2 regulates basolateral-to-apical transcytosis and lumen formation in association with Cdc42 and MAL2. Dev Cell *18*, 814-827.

Mellor, H. (2010). The role of formins in filopodia formation. Biochim Biophys Acta *1803*, 191-200.

Morel, E., Parton, R.G., and Gruenberg, J. (2009). Annexin A2-dependent polymerization of actin mediates endosome biogenesis. Dev Cell *16*, 445-457.

Nakano, K., Kuwayama, H., Kawasaki, M., Numata, O., and Takaine, M. (2010). GMF is an evolutionarily developed Adf/cofilin-super family protein involved in the Arp2/3 complex-mediated organization of the actin cytoskeleton. Cytoskeleton (Hoboken) *67*, 373-382.

Okada, K., Bartolini, F., Deaconescu, A.M., Moseley, J.B., Dogic, Z., Grigorieff, N., Gundersen, G.G., and Goode, B.L. (2010). Adenomatous polyposis coli protein nucleates actin assembly and synergizes with the formin mDia1. J Cell Biol.

Padrick, S.B., Cheng, H.C., Ismail, A.M., Panchal, S.C., Doolittle, L.K., Kim, S., Skehan, B.M., Umetani, J., Brautigam, C.A., Leong, J.M., *et al.* (2008). Hierarchical regulation of WASP/WAVE proteins. Mol Cell *32*, 426-438.

Paul, A.S., and Pollard, T.D. (2009). Energetic requirements for processive elongation of actin filaments by FH1FH2-formins. J Biol Chem *284*, 12533-12540.

Pollard, T.D. (2010). Mechanics of cytokinesis in eukaryotes. Curr Opin Cell Biol *22*, 50-56.

Qualmann, B., and Kessels, M.M. (2009). New players in actin polymerization--WH2-domain-containing actin nucleators. Trends Cell Biol *19*, 276-285.

Quinlan, M.E., Hilgert, S., Bedrossian, A., Mullins, R.D., and Kerkhoff, E. (2007). Regulatory interactions between two actin nucleators, Spire and Cappuccino. J Cell Biol *179*, 117-128.

Rebowski, G., Boczkowska, M., Hayes, D.B., Guo, L., Irving, T.C., and Dominguez, R. (2008). X-ray scattering study of actin polymerization nuclei assembled by tandem W domains. Proc Natl Acad Sci U S A *105*, 10785-10790.

Robertson, A.S., Smythe, E., and Ayscough, K.R. (2009). Functions of actin in endocytosis. Cell Mol Life Sci *66*, 2049-2065.

Romer, W., Pontani, L.L., Sorre, B., Rentero, C., Berland, L., Chambon, V., Lamaze, C., Bassereau, P., Sykes, C., Gaus, K., *et al.* (2010). Actin dynamics drive membrane reorganization and scission in clathrin-independent endocytosis. Cell *140*, 540-553.

Romero, S., Didry, D., Larquet, E., Boisset, N., Pantaloni, D., and Carlier, M.F. (2007). How ATP hydrolysis controls filament assembly from profilin-actin: implication for formin processivity. J Biol Chem *282*, 8435-8445.

Rosenblatt, J., Cramer, L.P., Baum, B., and McGee, K.M. (2004). Myosin II-dependent cortical movement is required for centrosome separation and positioning during mitotic spindle assembly. Cell *117*, 361-372.

Rouiller, I., Xu, X.P., Amann, K.J., Egile, C., Nickell, S., Nicastro, D., Li, R., Pollard, T.D., Volkmann, N., and Hanein, D. (2008). The structural basis of actin filament branching by the Arp2/3 complex. J Cell Biol *180*, 887-895.

Sakata, D., Taniguchi, H., Yasuda, S., Adachi-Morishima, A., Hamazaki, Y., Nakayama, R., Miki, T., Minato, N., and Narumiya, S. (2007). Impaired T lymphocyte trafficking in mice deficient in an actin-nucleating protein, mDia1. J Exp Med *204*, 2031-2038.

Schuh, M., and Ellenberg, J. (2008). A new model for asymmetric spindle positioning in mouse oocytes. Curr Biol *18*, 1986-1992.

Shi, Y., Zhang, J., Mullin, M., Dong, B., Alberts, A.S., and Siminovitch, K.A. (2009). The mDial formin is required for neutrophil polarization, migration, and activation of the LARG/RhoA/ROCK signaling axis during chemotaxis. J Immunol *182*, 3837-3845.

Skau, C.T., Neidt, E.M., and Kovar, D.R. (2009). Role of tropomyosin in formin-mediated contractile ring assembly in fission yeast. Mol Biol Cell *20*, 2160-2173.

Steffen, A., Faix, J., Resch, G.P., Linkner, J., Wehland, J., Small, J.V., Rottner, K., and Stradal, T.E. (2006). Filopodia formation in the absence of functional WAVE- and Arp2/3-complexes. Mol Biol Cell *17*, 2581-2591.

Svitkina, T.M., Bulanova, E.A., Chaga, O.Y., Vignjevic, D.M., Kojima, S., Vasiliev, J.M., and Borisy, G.G. (2003). Mechanism of filopodia initiation by reorganization of a dendritic network. J Cell Biol *160*, 409-421.

Urban, E., Jacob, S., Nemethova, M., Resch, G.P., and Small, J.V. (2010). Electron tomography reveals unbranched networks of actin filaments in lamellipodia. Nat Cell Biol *12*, 429-435.

Vavylonis, D., Wu, J.Q., Hao, S., O'Shaughnessy, B., and Pollard, T.D. (2008). Assembly mechanism of the contractile ring for cytokinesis by fission yeast. Science *319*, 97-100.

Watanabe, S., Ando, Y., Yasuda, S., Hosoya, H., Watanabe, N., Ishizaki, T., and Narumiya, S. (2008). mDia2 induces the actin scaffold for the contractile ring and stabilizes its position during cytokinesis in NIH 3T3 cells. Mol Biol Cell *19*, 2328-2338.

Watanabe, S., Okawa, K., Miki, T., Sakamoto, S., Morinaga, T., Segawa, K., Arakawa, T., Kinoshita, M., Ishizaki, T., and Narumiya, S. (2010). Rho and Anillin-dependent Control of mDia2 Localization and Function in Cytokinesis. Mol Biol Cell.

Yang, C., Czech, L., Gerboth, S., Kojima, S., Scita, G., and Svitkina, T. (2007). Novel roles of formin mDia2 in lamellipodia and filopodia formation in motile cells. PLoS Biol *5*, e317.

Yonetani, A., and Chang, F. (2010). Regulation of cytokinesis by the formin cdc12p. Curr Biol *20*, 561-566.

Zuchero, J.B., Coutts, A.S., Quinlan, M.E., Thangue, N.B., and Mullins, R.D. (2009). p53-cofactor JMY is a multifunctional actin nucleation factor. Nat Cell Biol *11*, 451-459.

CHAPTER 2

An actin-filament-binding interface on the Arp2/3 complex is critical for nucleation and branch stability

Note: The majority of information presented in this chapter was included in the publication:

Goley, E.D., Rammohan, A., Znameroski, E.A., Firat-Karalar, E.N., Sept, D., Welch, M.D. (2010) "An actin-filament-binding interface on the Arp2/3 complex is critical for nucleation and branch stability." Proc Natl Acad Sci U S A *107*, 8159-8164.

Introduction

The actin cytoskeleton plays an essential role in diverse cellular processes ranging from motility to division. A key control point in the cycle of actin filament (F-actin) assembly is the rate-limiting nucleation step, which can be accelerated in a regulated manner by the action of nucleating factors. One of the major actin-nucleating factors in cells is the Arp2/3 complex, a protein complex that consists of seven subunits including the actin-related proteins (Arp) Arp2 and Arp3 and the additional Arp2/3 complex (ARPC) polypeptides ARPC1-ARPC5. The Arp2/3 complex has been conserved during the evolution of most eukaryotic cells, and plays an important functional role in cell migration, endocytosis, phagocytosis and pathogen infection (Goley and Welch, 2006).

On its own the Arp2/3 complex is inactive, but it is activated to polymerize actin by binding to proteins called nucleation-promoting factors (NPFs) (Goley and Welch, 2006) as well as to ATP (Dayel et al., 2001; Le Clainche et al., 2001). Moreover, the nucleating activity of the Arp2/3 complex is stimulated by binding to F-actin (Higgs et al., 1999; Machesky et al., 1999), a phenomenon that results in autocatalytic actin assembly (Pantaloni et al., 2000). Once activated, the complex nucleates the polymerization of daughter filaments that emerge from the sides of mother filaments in a stereotypical Y-branch orientation with an approximate branch angle of 70˚ (Amann and Pollard, 2001; Blanchoin et al., 2000; Mullins et al., 1998). Such Arp2/3-containing branched structures have been observed in the actin network within lamellipodia at the leading edge of motile cells (Svitkina and Borisy, 1999). This branched filament geometry is proposed to be particularly suited for harnessing actin polymerization to generate motile force (Mogilner, 2006).

Atomic-resolution structures of the Arp2/3 complex with and without bound nucleotide and inhibitors have been determined (Nolen et al., 2004; Nolen and Pollard, 2007; Nolen et al., 2009; Robinson et al., 2001). Moreover, structural models of the Y-branch junction have been constructed using electron microscopy (Egile et al., 2005; Volkmann et al., 2001), culminating in a 2.6 nm resolution 3D model derived from docking crystal structures of Arp2/3 complex and actin into a reconstruction from electron tomography (Rouiller et al., 2008). In this model, Arp2 and Arp3 interact with the pointed end of the daughter filament, and all seven subunits contact the mother filament. ARPC2 and ARPC4 comprise the major mother filament-binding interface, consistent with earlier data from chemical crosslinking (Mullins et al., 1997), Arp2/3 complex reconstitution (Gournier et al., 2001) and antibody-inhibition experiments (Bailly et al., 2001). However, despite advances in our understanding of Y-branch structure, the functional importance of Arp2/3 complex residues implicated in mother-filament binding has not been extensively tested apart from an analysis of ARPC2 (*arc35*) mutants in *Saccharomyces cerevisiae*, which demonstrated an important role for ARPC2 residues in Arp2/3 complex nucleating activity in vitro and in growth and endocytosis in vivo (Daugherty and Goode, 2008).

To generate an independent structural model of the interaction between the ARPC2 and ARPC4 subunits of the Arp2/3 complex and the side of the mother filament, our collaborators David Sept and Aravind Rammohan

performed molecular dynamics and protein-protein dynamics simulations with both binding partners (Goley et al., 2010). Based on this analysis, a model of the ARPC2/ARPC4 interaction with F-actin was derived that corresponded remarkably well with previous models of the Arp2/3 complex in the Y-branch derived from electron microscopy (Rouiller et al., 2008). We used information from both the protein-protein docking and electron microscopy models to identify candidate amino acid residues that constitute a predicted actin-binding surface on ARPC2/ARPC4. To test the functional importance of these residues for the biochemical properties of the Arp2/3 complex, we mutated them and examined the mutant complexes for their ability to nucleate and bind to F-actin and form Y-branches. Using this approach, we determined that binding of the Arp2/3 complex to F-actin is crucial for actin nucleation and maintaining the stability of Y-branches.

Experimental Procedures

Baculovirus strain construction

Baculovirus strains expressing untagged recombinant human Arp2/3 subunits, as well as strains expressing p40-Flag-His_6, p21-CFP, and p40-YFP were generated as described previously (Goley et al., 2004; Gournier et al., 2001). Point mutations in ARPC2 and ARPC4 were made using the QuikChange Site-Directed Mutagenesis Kit (Stratagene) following the manufacturer's protocol. The DNA sequence of each construct was verified, and then baculovirus strains were prepared according to the procedures supplied with the Bac-to-Bac system (Invitrogen).

Protein expression and purification

Recombinant Arp2/3 complexes were expressed by infecting Hi5 cells with baculovirus strains expressing all Arp2/3 subunits including p40-Flag-His_6, as described previously (Goley et al., 2004). Arp2/3 complexes were purified by Ni-NTA chromatography (QIAGEN) followed by cation exchange chromatography on HiTrap SP (GE Biosciences) for most complexes, or by anion exchange chromatography on HiTrap Q (GE Biosciences) for those complexes containing p40-YFP. Ion exchange chromatography was followed by gel filtration (Superdex 200, GE Biosciences) into gel filtration buffer (20 mM MOPS pH 7.0, 100 mM KCl, 2 mM $MgCl_2$, 5 mM EGTA, 1 mM EDTA, 0.5 mM DTT, 0.2 mM ATP, 10% glycerol).

GST-WASP-WCA (residues 422 to 502 of human WASP) and GST-WASP-CA (residues 441 to 502) fusion proteins were expressed in *E. coli* BL21 (DE3) as described previously (Yarar et al., 2002). These proteins were purified by glutathione affinity chromatography (glutathione sepharose 4B, GE Biosciences) and then by gel filtration chromatography (Superdex 200, GE Biosciences) into gel filtration buffer. Protein was frozen in liquid nitrogen and stored at –80°C.

Arp2/3 complex activity assays

Actin co-pelleting assays were performed as described previously using 50 nM Arp2/3 complexes and the indicated concentrations of F-actin (Gournier et al., 2001). Curve fitting and K_d determination was performed using Prism software (GraphPad Software).

Debranching assays were performed essentially as described previously (Martin et al., 2006). Briefly, pyrene actin assembly assays were performed as described previously (Gournier et al., 2001) with wild-type (5 or 10 nM) or DKK mutant Arp2/3 complex (60 or 120 nM) and 200 nM GST-WASP-WCA. Samples were extracted at the indicated timepoints and filaments were immediately stabilized by addition of rhodamine phalloidin (Invitrogen Molecular Probes). The first time point (t = 0) was taken when actin polymerization reached steady state. Rhodamine-phalloidin-stabilized filaments were applied to poly-lysine coated cover slips and imaged using an Olympus BX51 microscope equipped with a 60X objective and a Hamamatsu Orca-ER camera. Images were captured in TIFF format using μManager software, and the frequency of branching was quantified by manual counting using Metamorph software (Molecular Devices). Images were prepared for presentation by adjusting brightness and contrast using Adobe Photoshop. Curve-fitting and Y-branch $t_{1/2}$ calculations were performed using Prism software (GraphPad Software).

Results

Charged surface residues on ARPC2 and APRC4 are critical for Arp2/3 complex-mediated actin nucleation

Protein-protein docking simulations carried out by our collaborators David Sept and Aravind Rammohan yielded a structural model of ARPC2/ARPC4 heterodimer bound to F-actin (Fig. 2.1A). This model was used to identify candidate surface residues on ARPC2/ARPC4 that are predicted to interact with F-actin. Some of these residues were also proposed to be involved in mother-filament binding by a homology modeling study that identified highly conserved amino acids within the Arp2/3 complex (Beltzner and Pollard, 2004) (Fig. 2.1A).

To test the functional importance of charged surface residues on ARPC2 and ARPC4, we mutated clusters of these residues to alanine, generating total of 11 mutant complexes that contained substitutions in 21 different amino acid residues. Each of the mutant complexes was expressed in insect cells using the baculovirus expression system and purified to homogeneity. None of the mutations had an effect on the stability or assembly of the complex, as each purified complex was obtained with similar yield and had the appropriate subunit stoichiometry.

We then assessed each purified complex for its ability to promote actin polymerization using the pyrene-actin assembly assay. Because Arp2/3-mediated actin nucleation is autocatalytic, we expected that mutations affecting F-actin binding would decrease activity. Of the 11 mutants tested, 3 exhibited

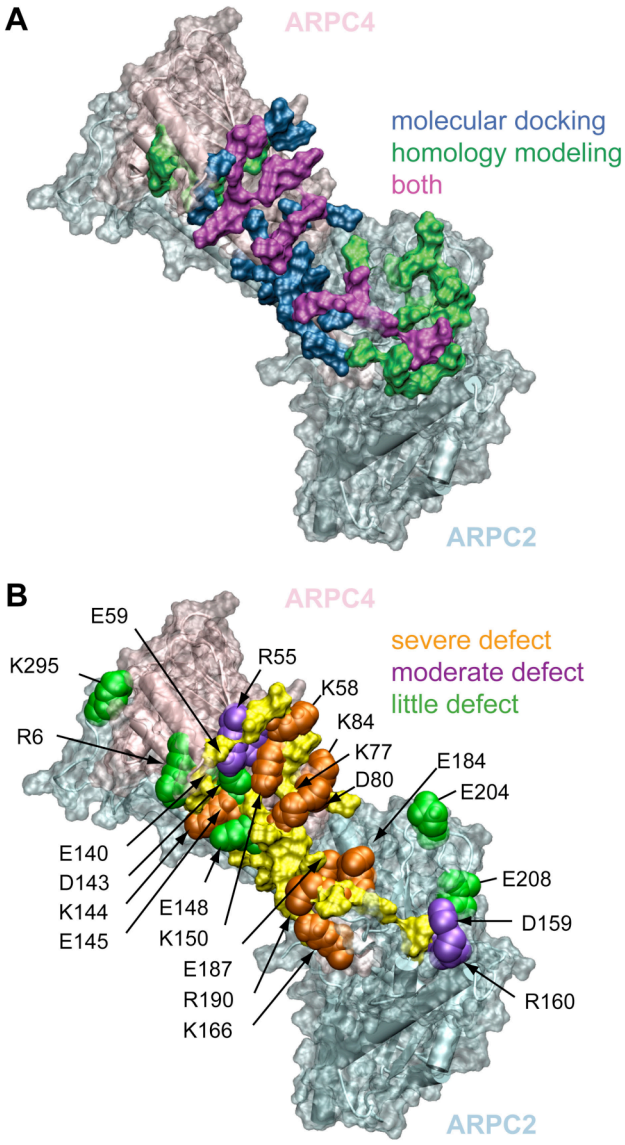

Figure 2.1: Residues on ARPC2 and ARPC4 identified by molecular docking and homology modeling lie on the surface that is critical for Arp2/3 complex activity

(A) Surface rendering showing the location of amino acid residues selected for mutagenesis (opaque and color coded) based on molecular docking (blue), homology modeling (green) or both (magenta).

(B) Surface rendering showing the correlation between the location of mutations on the surface of ARPC2/ARPC4 and the severity of the actin nucleation defects. The surface that is predicted to be within 4 Å of actin by protein-protein docking is opaque and yellow, and the side chains of mutated amino acids are shown in space filling representation and are color coded as follows: orange = severely defective, purple = moderately defective, and green = unaffected.

Mutations (shorthand designation)	Nucleation activity relative to wild-type*	Phenotypic designation
ARPC4-D143A K144A K150A (4DKK)	0.08 ± 0.02	severe
ARPC4-K58A K77A K84A (4KKK)	0.16 ± 0.05	severe
ARPC2-E187A R190A (2ER)	0.22 ± 0.02	severe
ARPC4-K166A/ARPC2-E184A (2E4K)	0.25 ± 0.06	severe
ARPC4-K77A D80A (4KD)	0.22 ± 0.02	severe
ARPC2-E184A E187A R190A (2EER)	0.33 ± 0.06	severe
ARPC2-D159A R160A (2DR)	0.56 ± 0.07	moderate
ARPC4-R55A E59A (4RE)	0.63 ± 0.11	moderate
ARPC4-E148A/ARPC2-K295A (2K4E)	0.87 ± 0.08	wild type
ARPC2-E204A E208A (2EE)	0.93 ± 0.14	wild type
ARPC4-R6A E140A D143A (4RED)	1.03 ± 0.13	wild type
Wild type	1.0	

Table 2.1: Summary of mutant complexes and their biochemical activities

Barbed ends generated by the indicated mutant complexes were normalized to barbed ends generated by wild-type Arp2/3 complex at the same concentration. Normalized activity was calculated for 5 nM, 20 nM, 50 nM, and 100 nM Arp2/3 complexes, and the mean±standard deviation of the activities at different concentrations is listed.

near-wild-type activity, and the remaining 8 exhibited nucleation defects ranging from 2-fold to 12-fold relative to wild-type (Table 2.1). These data indicate that numerous charged residues on the surface of ARPC2 and ARPC4 play a critical role in Arp2/3-complex-mediated actin polymerization.

We next examined the relationship between the location of each mutation on the surface of ARPC2/ARPC4 and the severity of the nucleation defect. Strikingly, when the mutations were mapped onto the surface, there was a clear spatial clustering by activity level (Fig. 2.1B). Mutations that caused moderate to severe biochemical defects clustered on the predicted binding interface with F-actin, and the least severe mutations scattered at the periphery or outside the predicted interface. Thus the locations of mutations that influence actin polymerization support the protein-protein docking models for the interaction of ARPC2 and ARPC4 with the mother filament.

Because the ARPC2 and ARPC4 subunits of the Arp2/3 complex have been predicted to form the major mother-filament-binding interface, we hypothesized that the mutations in residues that compromised actin polymerization activity did so by reducing the affinity for F-actin. Because the 4DKK mutant had the most severe defect in actin nucleation (Table 2.1), we selected it for further analysis. To measure the affinity for actin filaments, we performed actin copelleting asssays at a range of F-actin concentrations to measure (Fig. 2.2). The affinity of the 4DKK mutant for F-actin (K_d = 7.8 ± 3.7 μM; mean ± standard error of the mean) was 6 times lower than wild type (K_d = 1.3 ± 0.6 μM). This strongly suggests that the reduced polymerizing activity of 4DKK is due to a reduced affinity for actin filamentsThe same is likely to be true for the other mutants in the predicted actin-binding interface that have compromised actin nucleating activity.

The F-actin binding surface on ARPC2/ARPC4 is critical for Y-branch stability

To test whether the affinity of the Arp2/3 complex for F-actin affects its Y-branching activity, we compared the activity of the wild type complex and the 4DKK mutant with regard to Y-branch formation and stability. After controlling for the 12-fold difference in actin nucleating activity, we found that wild type and 4DKK formed a similar percentage of branched filaments (10 nM wild type formed 15 ± 3 % branched filaments (mean ± SEM); 120 nM 4DKK formed 13 ± 1 % branched filaments), and branch morphology was similar between wild type and mutant (Fig. 2.3A). This suggests that the lower affinity of the 4DKK mutant for F-actin results in lower nucleation and Y-branching activity, but nevertheless its nucleating and Y-branching activities remain tightly coupled as has been shown previously for wild type Arp2/3 complex (Higgs et al., 1999; Martin et al., 2006; Pantaloni et al., 2000). In addition to measuring Y-branch formation, we also measured Y-branch stability by initiating nucleation/branching reactions, fixing branches with rhodamine-phalloidin at various times post initiation, and quantifying branch frequency as a function of time (Fig. 2.3B). Wild type branches dissociated with a $t_{1/2}$ (half life) of 28 min, similar to previous reports (Martin et al., 2006). In contrast, branches formed by the 4DKK mutant

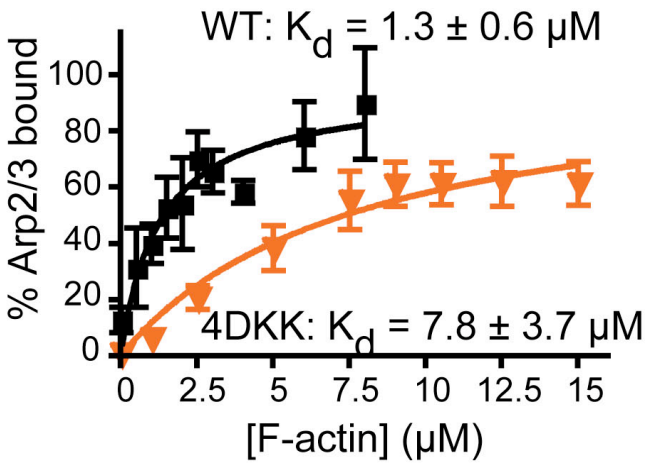

Figure 2.2: The 4DKK mutant is defective in binding to actin filaments

Percentage of WT (black) or 4DKK (orange) Arp2/3 complex found in the pellet fraction after high-speed centrifugation over a range of actin concentrations. Dissociation constants (K_ds) calculated from the resulting curves are indicated. Data are the mean ± SEM (n=6).

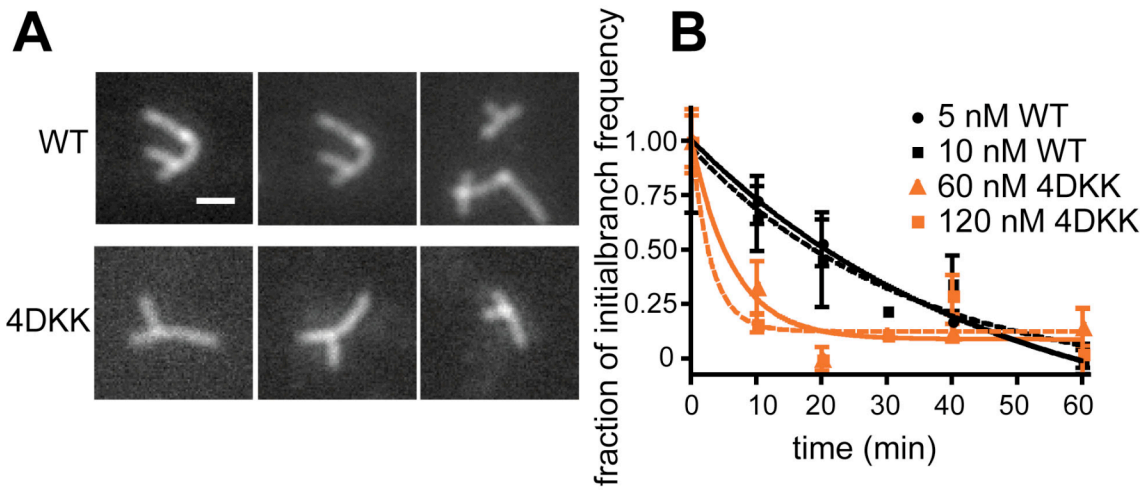

Figure 2.3: The 4DKK mutant forms short-lasting branches with normal morphology

(A) Images of branches formed by WT and the 4DKK complexes. Scale bar 2μm.

(**B)** Graph of the fraction of the initial branching frequency (normalized such that the branch frequency at t=0 is 1) versus time after initiating nucleation and branching for WT (black) and 4DKK (orange). Data are the mean ± SEM (n=3).

dissociated with a much shorter $t_{1/2}$ of <10 min. This indicates that residues within the ARPC2/ARPC4 heterodimer that affect the affinity of the Arp2/3 complex for F-actin are crucial for Y-branch stability.

Discussion

F-actin binding is critical to the nucleating and branching activities of the Arp2/3 complex. However, the molecular details of the interaction between the Arp2/3 complex and the mother filament, as well as the mechanism by which filaments stimulate the activity of the complex, are poorly understood. Previous models of the Arp2/3 complex in the Y-branch derived from electron microscopy identified ARPC2/ARPC4 as the major mother-filament-binding surface (Egile et al., 2005; Rouiller et al., 2008; Volkmann et al., 2001). In this study, we mutated surface residues on ARPC2 and ARPC4 that are predicted by protein-protein docking simulations and homology modeling studies to be important for F-actin binding. By examining the biochemical properties of mutant Arp2/3 complexes, we defined sites on ARPC2/ARPC4 that are required for high affinity binding to F-actin, efficient actin nucleation and Y-branching, and stability of Y-branches.

Mutating surface residues that span the predicted actin-binding surface on ARPC2/ARPC4 caused moderate to severe defects in actin polymerization. When we mapped the residues critical for actin nucleation onto the structure of the predicted interface between ARPC2/ARPC4 and F-actin, there was a striking correlation between the severity of actin nucleation defects and the proximity of the mutated residues to the predicted actin binding interface. This supports the validity of the protein-protein docking model for the ARPC2/ARPC4 F-actin interaction. It is important to note that the results of our mutagenesis experiments agree with a previous analysis of the phenotypes caused by mutating evolutionarily-conserved and solvent-exposed residues in *Saccharomyces cerevisiae* ARPC2 (Daugherty and Goode, 2008). In particular, mutating several residues that are conserved between yeast and human ARPC2 caused correspondingly mild (yeast *arc35-107*; human 2EE; E204A), moderate (yeast *arc35-104*; human 2DR; D159A R160A) and severe (yeast *arc35-106*; human 2ER, 2EER; E187A R190A) defects in actin nucleation. Our results demonstrate that the functional roles of these residues are conserved across species, and extend this analysis to examine the role of adjacent residues in ARPC4.

F-actin binding is tightly coupled to the nucleating activity of the Arp2/3 complex, suggesting that the nucleation defects observed for the mutant complexes might be due to defects in F-actin binding. Detailed examination of a severely defective mutant in ARPC4 (4DKK) in actin co-pelleting assays revealed that this mutant has 6-fold lower binding affinity for F-actin than the wild-type complex. This suggests that this surface of ARPC4 (and by extension the adjacent surface on ARPC2) is crucial for high affinity binding to F-actin. Although the remainder of the mutants that exhibit nucleation defects have not been characterized for their F-actin binding affinity, we expect that the severity of their nucleation defectswill correlate with their F-actin binding affinity, and analysis of these mutants will be important for fine mapping of the surface residues that mediate the interaction between the Arp2/3 complex and F-actin.

In addition to nucleation, binding of the Arp2/3 complex to the sides of actin filaments is central to its Y-branching activity. Although the precise mechanism of Arp2/3 complex activation by F-actin remains unclear, mathematical simulations suggest that an activation reaction occurs after actin binding, and that this is the rate-limiting step leading to branch formation (Beltzner and Pollard, 2008). Besides their role in promoting high affinity actin binding, residues on the surface of ARPC2/ARPC4 may also participate in this reaction. Once activation occurs, our data suggests that Y-branches form with normal geometry even when residues on ARPC2/ARPC4 are mutated. However, our results also indicate that residues in ARPC2/ARPC4 are crucial for maintaining the stability of the Y-branch, as the 4DKK mutant undergoes much more rapid branch dissociation than wild type Arp2/3 complex. These data suggest that residues on this surface of ARPC2/ARPC4 that are crucial for F-actin binding are also important for maintaining Y-branch stability, and that the affinity of the Arp2/3 complex for F-actin independently modulates branch formation and stability.

Our results have identified surface residues on the Arp2/3 complex that are important for its nucleating, F-actin binding and branching activities. This provides a more detailed picture of the nature of the molecular interactions between the Arp2/3 complex and F-actin. In addition to the key role played by ARPC2 and ARPC4 in this interaction, results from electron microscopy suggest that each of the remaining five subunits of the Arp2/3 complex makes contact with the mother filament (Rouiller et al., 2008), indicating that other interactions are also likely to be relevant in the intact complex. In the future, mutagenesis of the predicted binding surfaces on other subunits of the Arp2/3 complex, and subsequent biochemical characterization of the mutant complexes, will be important for obtaining a complete molecular picture of Arp2/3 complex bound to F-actin. Defining key functional residues on the Arp2/3 complex will also be valuable to address the importance of actin filament Y-branching by the Arp2/3 complex *in vivo*, as well as the mechanism by which filament binding promotes Arp2/3 activation.

References

Amann, K.J., and Pollard, T.D. (2001). Direct real-time observation of actin filament branching mediated by Arp2/3 complex using total internal reflection fluorescence microscopy. Proc Natl Acad Sci U S A *98*, 15009-15013.

Bailly, M., Ichetovkin, I., Grant, W., Zebda, N., Machesky, L.M., Segall, J.E., and Condeelis, J. (2001). The F-actin side binding activity of the Arp2/3 complex is essential for actin nucleation and lamellipod extension. Curr Biol *11*, 620-625.

Beltzner, C.C., and Pollard, T.D. (2004). Identification of functionally important residues of Arp2/3 complex by analysis of homology models from diverse species. J Mol Biol *336*, 551-565.

Beltzner, C.C., and Pollard, T.D. (2008). Pathway of actin filament branch formation by Arp2/3 complex. J Biol Chem *283*, 7135-7144.

Blanchoin, L., Amann, K.J., Higgs, H.N., Marchand, J.B., Kaiser, D.A., and Pollard, T.D. (2000). Direct observation of dendritic actin filament networks nucleated by Arp2/3 complex and WASP/Scar proteins. Nature *404*, 1007-1011.

Daugherty, K.M., and Goode, B.L. (2008). Functional surfaces on the p35/ARPC2 subunit of Arp2/3 complex required for cell growth, actin nucleation, and endocytosis. J Biol Chem *283*, 16950-16959.

Dayel, M.J., Holleran, E.A., and Mullins, R.D. (2001). Arp2/3 complex requires hydrolyzable ATP for nucleation of new actin filaments. Proc Natl Acad Sci U S A *98*, 14871-14876.

Egile, C., Rouiller, I., Xu, X.P., Volkmann, N., Li, R., and Hanein, D. (2005). Mechanism of filament nucleation and branch stability revealed by the structure of the Arp2/3 complex at actin branch junctions. PLoS Biol *3*, e383.

Goley, E.D., Rammohan, A., Znameroski, E.A., Firat-Karalar, E.N., Sept, D., and Welch, M.D. (2010). An actin-filament-binding interface on the Arp2/3 complex is critical for nucleation and branch stability. Proc Natl Acad Sci U S A *107*, 8159-8164.

Goley, E.D., Rodenbusch, S.E., Martin, A.C., and Welch, M.D. (2004). Critical conformational changes in the Arp2/3 complex are induced by nucleotide and nucleation promoting factor. Mol Cell *16*, 269-279.

Goley, E.D., and Welch, M.D. (2006). The ARP2/3 complex: an actin nucleator comes of age. Nat Rev Mol Cell Biol *7*, 713-726.

Gournier, H., Goley, E.D., Niederstrasser, H., Trinh, T., and Welch, M.D. (2001). Reconstitution of human Arp2/3 complex reveals critical roles of individual subunits in complex structure and activity. Mol Cell *8*, 1041-1052.

Higgs, H.N., Blanchoin, L., and Pollard, T.D. (1999). Influence of the C terminus of Wiskott-Aldrich syndrome protein (WASp) and the Arp2/3 complex on actin polymerization. Biochemistry *38*, 15212-15222.

Le Clainche, C., Didry, D., Carlier, M.F., and Pantaloni, D. (2001). Activation of Arp2/3 complex by Wiskott-Aldrich Syndrome protein is linked to enhanced binding of ATP to Arp2. J Biol Chem *276*, 46689-46692.

Machesky, L.M., Mullins, R.D., Higgs, H.N., Kaiser, D.A., Blanchoin, L., May, R.C., Hall, M.E., and Pollard, T.D. (1999). Scar, a WASp-related protein, activates nucleation of actin filaments by the Arp2/3 complex. Proc Natl Acad Sci U S A *96*, 3739-3744.

Martin, A.C., Welch, M.D., and Drubin, D.G. (2006). Arp2/3 ATP hydrolysis-catalysed branch dissociation is critical for endocytic force generation. Nat Cell Biol *8*, 826-833.

Mogilner, A. (2006). On the edge: modeling protrusion. Curr Opin Cell Biol *18*, 32-39.

Mullins, R.D., Heuser, J.A., and Pollard, T.D. (1998). The interaction of Arp2/3 complex with actin: nucleation, high affinity pointed end capping, and formation of branching networks of filaments. Proc Natl Acad Sci U S A *95*, 6181-6186.

Mullins, R.D., Stafford, W.F., and Pollard, T.D. (1997). Structure, subunit topology, and actin-binding activity of the Arp2/3 complex from Acanthamoeba. J Cell Biol *136*, 331-343.

Nolen, B.J., Littlefield, R.S., and Pollard, T.D. (2004). Crystal structures of actin-related protein 2/3 complex with bound ATP or ADP. Proc Natl Acad Sci U S A *101*, 15627-15632.

Nolen, B.J., and Pollard, T.D. (2007). Insights into the influence of nucleotides on actin family proteins from seven structures of Arp2/3 complex. Mol Cell *26*, 449-457.

Nolen, B.J., Tomasevic, N., Russell, A., Pierce, D.W., Jia, Z., McCormick, C.D., Hartman, J., Sakowicz, R., and Pollard, T.D. (2009). Characterization of two classes of small molecule inhibitors of Arp2/3 complex. Nature *460*, 1031-1034.

Pantaloni, D., Boujemaa, R., Didry, D., Gounon, P., and Carlier, M.F. (2000). The Arp2/3 complex branches filament barbed ends: functional antagonism with capping proteins. Nat Cell Biol *2*, 385-391.

Robinson, R.C., Turbedsky, K., Kaiser, D.A., Marchand, J.B., Higgs, H.N., Choe, S., and Pollard, T.D. (2001). Crystal structure of Arp2/3 complex. Science *294*, 1679-1684.

Rouiller, I., Xu, X.P., Amann, K.J., Egile, C., Nickell, S., Nicastro, D., Li, R., Pollard, T.D., Volkmann, N., and Hanein, D. (2008). The structural basis of actin filament branching by the Arp2/3 complex. J Cell Biol *180*, 887-895.

Svitkina, T.M., and Borisy, G.G. (1999). Arp2/3 complex and actin depolymerizing factor/cofilin in dendritic organization and treadmilling of actin filament array in lamellipodia. J Cell Biol *145*, 1009-1026.

Volkmann, N., Amann, K.J., Stoilova-McPhie, S., Egile, C., Winter, D.C., Hazelwood, L., Heuser, J.E., Li, R., Pollard, T.D., and Hanein, D. (2001). Structure of Arp2/3 complex in its activated state and in actin filament branch junctions. Science *293*, 2456-2459.

Yarar, D., D'Alessio, J.A., Jeng, R.L., and Welch, M.D. (2002). Motility determinants in WASP family proteins. Mol Biol Cell *13*, 4045-4059.

CHAPTER 3

JMY is an actin nucleator and Arp2/3 activator that functions in neuritogenesis

Introduction

The actin cytoskeleton plays essential roles in basic cellular processes including migration, adhesion and division (Pollard and Cooper, 2009), membrane trafficking events (Lanzetti, 2007) as well as in more specialized processes like neuritogenesis (Kessels et al., 2010). In the case of cell migration, dynamic actin polymerization in protrusive structures such as filopodia and lamellipodia generate the force that drives leading edge protrusion. Neuronal cells also rely on these membrane protrusions for the establishment of polarity, formation of growth cones and neurite extension during their development and differentiation. Understanding how the dynamic actin cytoskeleton contributes to these cellular processes will require a complete characterization of the regulators of actin polymerization.

Actin nucleation is the rate-limiting step in actin polymerization and is accelerated by three different classes of actin nucleators: the Arp2/3 complex and its activators - the nucleation promoting factors (NPFs), as well as formins and finally tandem-monomer-binding nucleators (Campellone and Welch, 2010; Firat-Karalar and Welch, 2010). Each has a distinct molecular mechanism of action and mode of regulation (Firat-Karalar and Welch, 2010). The junction-mediating and regulatory protein (JMY) was recently discovered as a new nucleator that acts as a hybrid of the first and third classes (Zuchero et al., 2009). Originally identified as a partner of the transcription co-activator p300, JMY was first shown to function in the p53 response by augmenting p53-dependent transcription and apoptosis (Shikama et al., 1999). Upon DNA damage, JMY is released from Mdm2, which targets it for ubiquitin-dependent degradation, and then accumulates in nucleus (Coutts et al., 2007). These functions are mediated by the N-terminal domain that is specific to JMY and central coiled-coil region. In addition, JMY has a highly conserved C-terminal WWWCA domain consisting of three tandem actin-binding WH2 domains (WWW) and Arp2/3-binding connector (C) and acidic (A) regions (Zuchero et al., 2009). The WWW domain of JMY nucleates unbranched actin filaments independently of the Arp2/3 complex by bringing together actin monomers to form a polymerization nucleus similar to the tandem-monomer-binding nucleator Spire. In addition, the WWWCA domain activates the Arp2/3 complex to promote the formation of Y-branched actin networks. Thus, JMY is unique among known actin nucleators in combining Arp2/3-dependent and Arp2/3–independent nucleating abilities within the same protein.

How the actin nucleating activity of JMY is regulated remains to be determined. The N-terminal domains of NPFs are highly divergent and were shown to differentially modulate the regulation and function of class I NPFs *in vivo* (Campellone and Welch, 2010). The canonical mode of regulation of NPFs involves modulating the accessibility of the WCA domain. For the NPFs WASP and N-WASP, the activity of the WCA domain is autoinhibited through intramolecular interactions between it and the upstream domains and this inhibition is relieved by the Rho family GTPases Cdc42 and Rac, PIP2 and SH3-containing proteins (Kim et al., 2000; Miki et al., 1998; Prehoda et al., 2000; Tomasevic et al., 2007). In contrast, the activity of the WCA domain in WAVEs is trans-inhibited by interacting proteins and activated by the Rho family GTPase

Rac (Derivery et al., 2009; Eden et al., 2002; Ismail et al., 2009; Lebensohn and Kirschner, 2009). Because the role of full-length JMY in actin assembly has not yet been determined, it is not clear whether JMY is regulated by a WASP-type, WAVE-type or other mechanism.

In keeping with its activity as an actin nucleator, JMY localizes to the leading edge of migrating cells and functions in cell motility by activating Arp2/3-complex-mediated actin polymerization (Zuchero et al., 2009), but also by antagonizing cellular adhesion through regulation of cadherin expression (Coutts et al., 2009). In addition, the intrinsic nucleating ability of JMY might be required for its function in the nucleus as a transcriptional co-activator (Coutts et al., 2009). Despite these advances in understanding the cellular functions of JMY, whether JMY plays a role in other actin-dependent cellular processes remains to be determined.

Here we investigated the activity of full-length JMY in actin assembly *in vitro*, and the cellular role of JMY in neurons. We found that full-length JMY and the truncated WWWCA region have comparable actin nucleating and Arp2/3-complex-activating abilities *in vitro*. However, compared with the WWWCA, the ability of full-length JMY to induce actin polymerization is significantly decreased in cells. This suggests potential mechanisms for JMY regulation. We also showed that the primary localization of JMY is in the cytosol in addition to its localization in the nucleus, and that it induces the formation of F-actin clusters in cells. Finally, we demonstrated a previously unidentified role for JMY in neurons, as a negative regulator of neurite outgrowth during neuronal differentiation.

Experimental Procedures

Plasmids

Plasmids are listed in table S1. The JMY coding sequence was amplified by PCR from full-length mouse JMY cDNA (accession BC090835, Open Biosystems) using primers listed in Table S2. The JMY-W981A point mutation was made using the QuikChange Site-Directed Mutagenesis Kit (Stratagene) in accordance with the manufacturer's instructions. The DNA sequence of each construct was verified.

Protein Expression and Purification

His-JMY, His-JMY (W981A), GST-JMY and rArp2/3 were expressed and purified using the baculovirus expression system. Sf9 and Hi5 insect cells were cultured at 28°C in Grace's medium supplemented with 2% FBS, penicillin and streptomycin. Bacmids and baculoviruses were generated using the Bac-to-Bac system according to the manufacturer's instructions (Invitrogen). Recombinant proteins were then expressed by infecting Hi5 cells for 72 h at 28°C with the appropriate baculovirus strains. Hi5 cells were pelleted, lysed by freeze-thaw in Ni-NTA lysis buffer (50 mM NaH_2PO_4 pH 8.0, 300 mM NaCl, 10 mM imidazole

Primers

Primer	Sequence 5 to 3' (R. E. Site in CAPS)	R. E. Site	Reference
ENF1	cgGAATTCttaatgtcgttcgcgctg	EcoRI	Current Study
ENF2	gcgGCGGCCGCctagttctcccagtc	NotI	Current Study
ENF3	attGCGGCCGCctagttctccgcgtc	NotI	Current Study
ENF4	gaAGATC Tatgtcgttcgcgctg	BglII	Current Study
ENF5	cgGAATTCctagttctcccagtc	EcoRI	Current Study
ENF6	cgGAATTCgttgcaaaggacaatgg	EcoRI	Current Study

R. E. = restriction enzyme

Plasmids

Plasmid	Vector	Tag	Species	Residues	R. E. Sites	Primers	Reference
Insect cell expression							
pFastBacHT-A	pFastBacHT-A	His6(N)	n/a	n/a	n/a	n/a	Invitrogen
pFB-JMY	pFastBacHT-A	His6(N)	n/a	1-983	EcoRI-NotI	1 + 2	Current Study
pFB-JMY(W981A)	pFastBacHT-A	His6(N)	mouse	1-983	EcoRI-NotI	1 + 3	Current Study
Bacterial expression							
pGEX4t-1	pGEX4t-1	GST(N)	n/a	n/a	pGEX4t-1	n/a	Phamacia
pGST-JMY WWWCA	pGEX4t-1	GST(N)	n/a	816-983	EcoRI-NotI	6 + 2	Current Study
pGST-JMY WWWCA (W981A)	pGEX4t-1	GST(N)	mouse	816-983	EcoRI-NotI	6 + 3	Current Study
Mammalian cell expression							
pEGFP-C1	pEGFP-C1	GFP(N)	n/a	n/a	pEGFP-C1	n/a	Clontech
pEGFP-JMY	pEGFP-C1	GFP(N)	mouse	1-983	EcoRI-NotI	1 + 2	Current Study
pEGFP-JMY WWWCA	pEGFP-C1	GFP(N)	mouse	816-983	EcoRI-NotI	6 + 2	Current Study
pKC-LAP-C1	PIC 113	HisGFP-S(N)	n/a	n/a	PIC 113	n/a	Campellone et al., 2008
pLAP-JMY	pKC-LAP-C1	HisGFP-S(N)	mouse	1-983	EcoRI-BglII	4 + 5	Current Study
pKC-MCH-C1	pEGFP-C1	mCherry(N)	n/a	n/a	pEGFP-C1	n/a	Campellone et al., 2008
pKC-MCH-JMY	pKC-MCH-C1	mCherry(N)	mouse	1-983	EcoRI-NotI	1 + 2	Current Study

N = N-terminal tag

Table 3.1: Primers and plasmids used in this study

and protease inhibitors (10μg/ml each of aprotinin, leupeptin, pepstatin, and 1 mM PMSF)) and clarified by centrifugation. His-JMY and His-JMY (W981A) were purified from the resulting supernatant by Ni-NTA chromatography (Qiagen) followed by anion exchange chromatography on a HiTrap QP column (GE Healthcare) and finally gel filtration chromatography on a Superdex 200 column (GE Healthcare) into gel filtration buffer (20 mM MOPS pH 7.0, 100 mM KCl, 2 mM $MgCl_2$, 5 mM EGTA, 1 mM EDTA, 0.5 mM DTT, 0.2 mM ATP, 10% glycerol, protease inhibitors). rArp2/3 complex was purified as described previously (Goley et al., 2004).

GST-JMY WCA, GST-JMY WCA (W981A) and GST-N-WASP WCA were expressed in *E. coli* BL21-Rosetta cells grown to OD_{600}= 0.6 and induced with 1 mM isopropyl β-D-1-thiogalactopyranoside (IPTG) for 4 h at 37°C. Following expression, bacteria were pelleted and lysed by freeze-thaw and sonication with 1 mg/ml lysozyme in GST-binding lysis buffer (1X PBS (137 mM NaCl, 2.7 mM KCl, 8 mM Na_2HPO_4, 1.46 mM KH_2PO_4) pH 7.4, 250 mM KCl, protease inhibitors). The proteins were purified by glutathione affinity chromatography (GE Healthcare) followed by gel filtration chromatography on a Superdex 75 column (GE Healthcare) into gel filtration buffer.

For affinity purification of recombinant JMY from mammalian cells, JMY was tagged with an N-terminal localization and affinity purification (LAP) tag (LAP-JMY) consisting of GFP, a TEV protease cleavage site and the S peptide portion of RNAse (Cheeseman and Desai, 2005). 293 cells were transfected with LAP-JMY and stable cell lines that express LAP-JMY were selected in 1 mg/ml G418. LAP-based purification was performed as described previously (Cheeseman and Desai, 2005) with the following modifications. Briefly, cells were lysed in lysis buffer (75 mM HEPES pH 7.5, 1.5 mM EGTA, 1.5 mM $MgCl_2$, 300 mM KCl, 15% glycerol, 0.4% NP-40, protease inhibitors) and LAP-JMY was first isolated from the cell extracts using protein A Sepharose beads (Amersham) coated with anti-GFP antibodies. Bound protein was eluted by cleaving with 0.06 mg/ml TEV protease in TEV cleavage buffer (50 mM HEPES, pH 7.5, 1 mM EGTA, 1 mM $MgCl_2$, 300 mM KCl, 10% glycerol, 0.05 % NP-40, 1 mM DTT). The supernatant after TEV cleavage contained S-JMY along with other binding proteins.

Antibody generation and immunoblotting

Polyclonal anti-JMY and anti-GFP antibodies were generated by immunizing rabbits (Covance) with full-length His-JMY or His-GFP, respectively. Antibodies were affinity purified using standard procedures (Harlow and Lane, 1988). Anti-JMY was used for immunoblotting at 1:4000. Other primary antibodies used for immunoblotting were anti-tubulin E7 (1:5000, developed by M. Klymkowsky at the University of Colorado, Boulder, maintained by the DSHB) and anti-NonO (1:4000, BD Biosciences). HRP-conjugated secondary antibodies were from GE Healthcare. For immunoblotting, extracts were resolved by SDS-PAGE and transferred onto nitrocellulose membranes that were then probed with primary and secondary antibodies and visualized by chemiluminescence (GE Healthcare). For

determining tissue-specific expression of JMY, a mouse tissue blot (Imgenex) was used.

Arp2/3 complex activity assays

Rabbit skeletal muscle actin and pyrene-labeled actin were prepared and pyrene actin polymerization assays were performed essentially as described previously (Goley et al., 2004). Pyrene actin and unlabeled actin were mixed in G-buffer (5 mM Tris pH 8.0, 0.2 mM $CaCl_2$, 0.2 mM ATP, 0.2 mM DTT) to generate a 3 μM G-actin solution with 7% pyrene-actin. 14 μl of reaction mixture containing proteins to be tested in the assay was mixed with 6 μl 10X initiation buffer (20 mM $MgCl_2$, 10 mM EGTA, 5 mM ATP), and this mixture was added to 40 μl of G-actin mix to start polymerization. Flourescence was detected at 20 s intervals at 365 nm excitation and 407 emission wavelengths on a Fluorolog-3 model FL3-11 spectrofluoremeter (Horiba Jobin Yvon). DataMax v2.2.12B software was used for data collection. Polymerization reactions were allowed to reach steady state, and curves were normalized for differences in steady-state fluorescence.

For the branching experiments, 3 μM actin mix was polymerized under the same conditions as those described for the pyrene actin polymerization assays. Samples were collected as soon as the polymerization reactions reached steady state and immediately stabilized with rhodamine-phalloidin (Invitrogen Molecular Probes). The stabilized filaments were diluted, applied to poly-(L)-lysine (Sigma) coated coverslips and imaged using an Olympus BX51 microscope equipped with a 60X objective and a Hamamatsu Orca-ER camera using μManager software (Edelstein et al., 2010). For each condition, branched and unbranched filaments in 10 different images were manually counted using Image J software (National Institutes of Health) in three separate experiments and the percent branching was calculated. A filament with more than one branch was counted as one. Image analysis and contrast adjustment was done using Adobe Photoshop.

Bead motility assays

For the bead motility experiments, polystyrene microspheres (Polysciences, 0.5 μm, non-functionalized) were incubated on ice with 1 μM GST-JMY WCA or GST-JMY WCA (W981A) for 1 h and then blocked with 5 mg/ml BSA for 15 min. Beads were washed and resuspendend in CSF-XB (10 mM HEPES pH 7.7, 2 mM $MgCl_2$, 0.1 mM $CaCl_2$, 100 mM KCl, 5 mM EGTA and 50 mM sucrose) and kept at 4 °C. Beads (1μl) were incubated with 1 μl actin (2 μM, 20% rhodamine-labelled) and 8 μl of *Xenopus laevis* egg extract (Maresca and Heald, 2006) and 2 μl of this reaction was squashed between a microscope slide and 22-mm-square glass coverslips, sealed and observed after 15-30 min using fluorescence and phase-contrast microscopy as described below.

Cell fractionation

For nuclear and cytosolic fractionation, cells were washed with PBS and lysed in cytosolic lysis buffer (10 mM HEPES pH 7.9, 10 mM KCl, 0.1 mM EDTA, 0.4 % NP-40, protease inhibitors) for 15 min on ice. The homogenate was then centrifuged at 3000 X g for 3 min to sediment the nuclei and the pellet was used to make the nuclear fraction. The supernatant was re-sedimented at 3000 X g for 5 min and the resulting supernatant was the cytosolic fraction. The nuclear pellet was washed with cytosolic lysis buffer, resuspended in nuclear lysis buffer (20 mM HEPES pH 7.9, 0.4 M NaCl, 1 mM EDTA, 10% glycerol, protease inhibitors) and sonicated on ice to extract nuclear proteins. The extracted material was sedimented at 15,000 X g for 5 min and the resulting supernatant was the nuclear fraction. The total protein yield of nuclear and cytosolic extracts was quantified using the Bradford assay. 30 μg of each extract was resolved by SDS-PAGE, blotted with anti-JMY antibodies and the intensity of JMY bands in each fraction were determined by densitometry using Adobe Photoshop. Relative JMY levels in the nuclear and cytoplasmic fractions were calculated by multiplying the intensities of JMY bands with the total amount of protein in each fraction. Relative JMY levels in nuclear and cytosolic extracts are presented as the mean +/- SEM of three independent experiments.

Mammalian cell culture, transfection and RNA interference

Cos7, U2OS, 293, HFF, WAVE2$^{+/+}$ and WAVE2$^{-/-}$ MEFs (Yan et al., 2003), SY5Y and Neuro 2a cells were cultured at 37°C in 5% CO_2 in DMEM (Invitrogen) supplemented with 10% Fetal Bovine Serum (FBS; JR Scientific), penicillin, and streptomycin. PC12 cells were cultured at 37°C in 5% CO_2 in RPMI 1640 (Invitrogen) supplemented with 10% FBS, penicillin, and streptomycin. For expression of recombinant tagged proteins, mammalian cells were transfected with the indicated DNA constructs using Lipofectamine LTX (Invitrogen) for Neuro 2a cells, and Lipofectamine 2000 (Invitrogen) for other cell lines, in accordance with the manufacturer's instructions. At 24 h post-transfection, cells were seeded onto glass coverslips for subsequent immunofluorescence experiments. To silence JMY expression by RNAi, Neuro 2a cells were transfected independently with 20 nM each of two different siRNAs (JMY siRNA#1:sc-35725, Santa Cruz Biotecnology and JMY siRNA#2: ID 75606, Ambion) using RNAiMAX (Invitrogen). For differentiation experiments, Neuro 2a cells at 24 h post-transfection were seeded onto glass coverslips coated with 1 mg/ml poly-(D)-lysine (Sigma) at a density 10^4 cels/cm^2.

For wound healing experiments, WAVE2$^{+/+}$ and WAVE2$^{-/-}$ cells were plated on glass-bottom plates (MatTek) that were marked to guide the localization of wounds. Cells were transfected with 20 nM control GAPDH siRNAor JMY siRNA#1 and were grown to confluency over 72 h. One day before wounding, cells were serum-starved in serum-free DMEM with 0.5% fetal bovine serum for 16 h. After serum starvation, three parallel wounds were made by scratching the cell monolayer with a 27G syringe. Cells were then washed with PBS to remove detached cells and replaced with fresh serum-starvation medium. Phase contrast images of 8 different wounds per sample were captured using an Olympus IX71 microscope with a 20 X (0.75 NA) PlanApo phase objective every 1.5 h over a period of 4.5 h (image acquisition described below). The wound area

at each time point was determined using ImageJ (Abramoff et al. 2004) and the percentage of wound closure was defined as the difference between the wound area at 0 h and the remaining wound area at 4.5 h. The data presented are the mean +/- SEM for three independent experiments.

Immunofluorescence microscopy, image acquisition and microscopic quantification

For immunofluorescence experiments, cells were washed with PBS, fixed in PBS with 2.5% paraformaldehyde for 30 min at 37ºC and permeabilized with 0.1% Triton X-100 for 5 min. They were then blocked with PBS with 1% BSA and 1% FBS and treated with 4 U/ml Alexa Fluor 488- or 568-phalloidin (Invitrogen) in PBS with 1%BSA. Coverslips were mounted on glass slides using ProLong Gold anti-fade reagent (Invitrogen).

Images were acquired using 20X (0.75 NA), 60X (1.40 NA) or 100X (1.35 NA) PlanApo objective lenses on a Olympus IX71 microscope equipped with a Photometrics Coolsnap HQ camera. Images were captured using Metamorph (Universel Imaging) or μManager (Edelstein et al., 2010) software, converted to 8-bit tiff files and brightness/contrast levels were adjusted using Adobe Photoshop. Quantification was done in a blinded fashion by scoring cells that were chosen randomly. Statistical significance and p values were assessed using ANOVA and Student's t tests using Prism software (GraphPad Software).

For quantification of relative F-actin levels in cells expressing GFP-JMY and GFP-JMY WCA, images of transfected and non-transfected cells in the same field were acquired as described above. Cell boundaries were outlined and the intensity of Alexa Fluor-568 phalloidin fluorescence was measured using Adobe Photoshop. F-actin fluorescence intensities from transfected cells were then normalized relative to that of nearby non-transfected cells that had a similar overall area. For images with more than one non-transfected cell, the average fluorescence intensity of these cells was used as the reference intensity for normalization.

Neurite initiation and morphological quantification

Following 24 h post-transfection with plasmids to express JMY or siRNA to silence its expression, Neuro 2a cells were induced to differentiate with 20 μM retinoic acid (RA) (Sigma) in DMEM with 2% FBS for 48 h and 72 h. The cells were quantified for the following parameters: percentage of cells with neurites, defined as an outgrowth with a length more than twice the diameter of the cell body; average neurite length, defined as the distance from cell body to the distal tip, measured using the NeuronJ plugin (Meijering et al., 2004) for ImageJ (Abramoff et al. 2004); average number of neurites per cell; and mean number of neurite branchpoints per unit neurite length for which branchpoints are defined as as secondary neurites of any length arising from the primary neurite. The data presented for the percentage of neurite-bearing cells are the mean +/- SEM for three independent experiments and at least 500 cells per transfection. The data presented for the rest of the quantifications are the mean +/- SEM of two independent experiments and at least 100 cells per transfection.

Results

Full-length JMY nucleates actin filaments and activates the Arp2/3 complex in vitro

JMY contains a unique N-terminal domain, three central coiled-coil domains, a polyproline region and a C-terminal WWWCA domain (Figure 1A). The isolated JMY WWWCA domain was previously shown to nucleate actin polymerization and promote Arp2/3 complex-mediated actin assembly (Zuchero et al., 2009), but the activity of the full-length JMY protein was not investigated. To determine whether full-length JMY affects actin assembly in vitro, we purified His-tagged full-length recombinant JMY (His-JMY) from insect cells, and for comparison, also purified GST-JMY-WWWCA from *E. coli* (Figure 1B). We then examined their ability to promote actin nucleation in the absence and presence of Arp2/3 complex using the pyrene-actin polymerization assay. Both His-JMY and GST-JMY-WWWCA induced rapid, dose-dependent actin polymerization in the absence of Arp2/3 complex, and their relative activities were similar (Figure 1C). In the presence of the Arp2/3 complex, actin polymerization by either His-JMY or GST-JMY-WWWCA was further accelerated. The Arp2/3-stimulating activity, but not the intrinsic actin nucleation activity, was disrupted by mutating a conserved tryptophan residue (W981) in the A domain, which was implicated in Arp2/3 complex binding and activation by all NPFs (Marchand et al., 2001). Together these results imply that full length JMY behaves very similarly to JMY-WWWCA in its actin-nucleating and Arp2/3 complex-activating activities.

To further examine the organization of actin filaments nucleated by full-length JMY in the absence and presence of the Arp2/3 complex, we visualized individual filaments in polymerization reactions with GST-JMY by fluorescence microscopy (Figure 1E and F). By itself, GST-JMY nucleated unbranched filaments, as described previously for JMY-WWWCA (Zuchero et al., 2009). In the presence of the Arp2/3 complex, GST-JMY stimulated the formation of Y-branches, albeit at a lower frequency that the GST-N-WASP WCA control. These results are consistent with its ability to activate Arp2/3-mediated actin polymerization.

Finally, we sought to examine the activity of JMY purified from mammalian cells to examine its potential mode of regulation. To this end, we generated a stable human epithelial kidney 293 cell line expressing JMY with an N-terminal localization and affinity purification (LAP) tag (Cheeseman and Desai, 2005) consisting of GFP and a TEV protease cleavage site, and an S peptide (Figure 2A). After the first step of purification using anti-GFP-antibody affinity followed by TEV cleavage, the S-JMY was purified from the stably-transfected cell line but not control untransfected cells (Figure 2B). Interestingly, no stoichiometric binding partners co-purified with JMY under these conditions, suggesting it may not be present in a stable complex in cells. We then compared the activity of JMY expressed in mammalian versus insect cells using the pyrene actin polymerization assay. JMY expressed in mammalian cells accelerated actin polymerization in the absence and presence of the Arp2/3 complex in a dose-dependent manner and had comparable activity to JMY expressed in insect cells (Figure 2C). This suggests that, under these conditions, full length JMY is fully

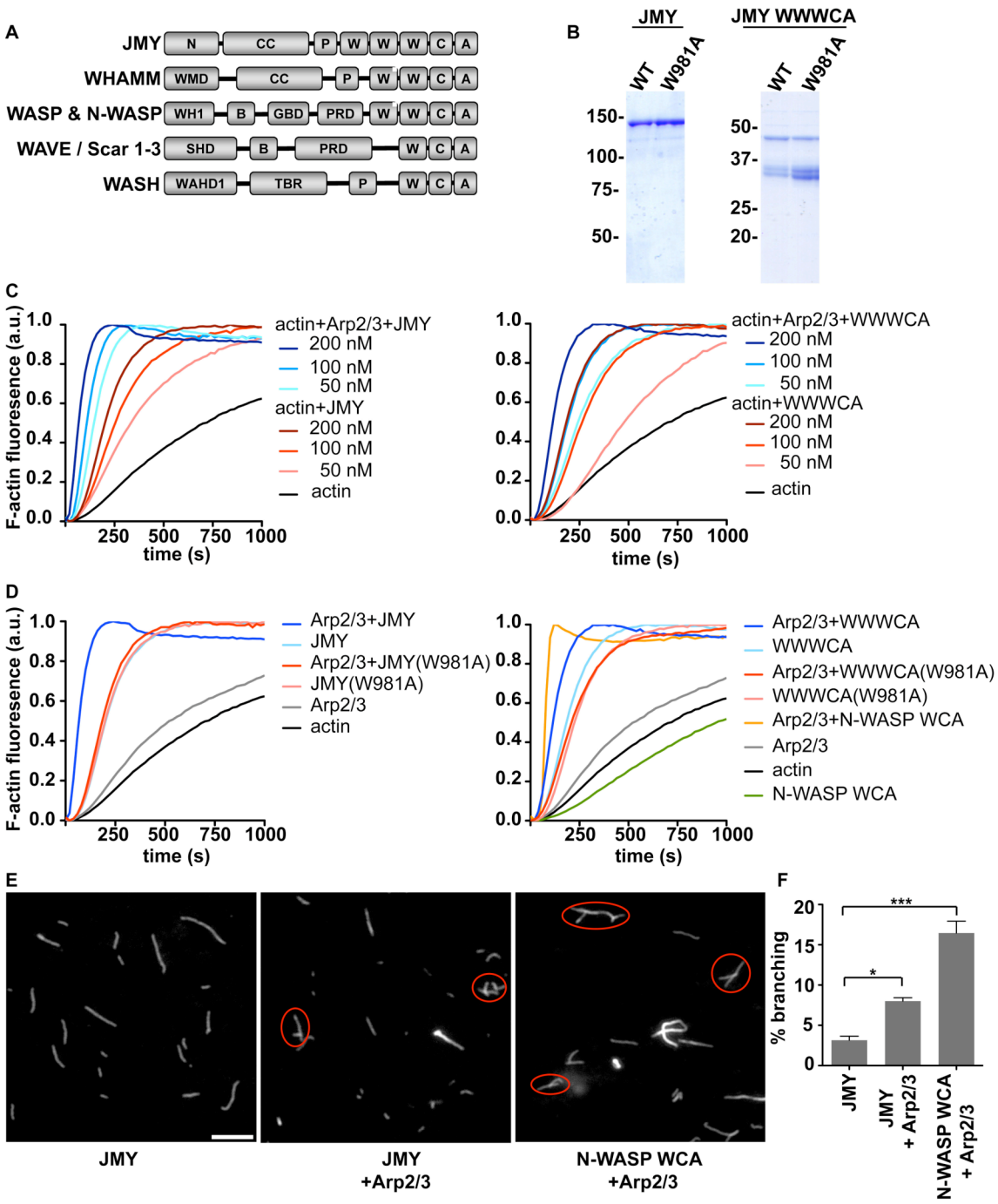

Figure 3.1: JMY and JMY-WWWCA are actin nucleators and nucleation promoting factors *in vitro*

(A) Domain organization of JMY and other NPFs are shown. Abbreviations: N: N-terminal domain, CC: coiled-coil region, P: polyproline region, W: WH2 domain, C: connector domain, A: acidic domain, WMD: WHAMM membrane interaction domain, B: basic domain, GBD: GTPase-binding domain, PRD:

proline-rich domain, SHD: Scar-homology domain, WAHD1: WASH homology domain 1, TBR: tubulin-binding region

(B) Purified His-JMY and GST-JMY-WWWCA were resolved by SDS-PAGE and stained with Coomassie blue.

(C) Actin (2μm, 7% pyrene labeled) was polymerized with the indicated concentrations of His-JMY or GST-JMY-WWWCA with or without 20 nm Arp2/3 complex.

(D) Actin (2μm, 7% pyrene-labeled) was polymerized with 200 nM His-JMY, His-JMY(W981A), GST-JMY-WWWCA, GST-JMY-WWWCA(W981A) or GST-N-WASP WCA with or without 20 nm Arp2/3 complex.

(E) Images of actin filaments (2 μM actin) polymerized by 200 nM GST-JMY or a GST-N-WASP-WCA control with or without 10 nM Arp2/3 complex. Scale bar 5 μm.

(F) Quantification of the percentage of branched filaments for the conditions described in (E). Data are the mean ± SEM of three experiments with at least 200 filaments manually counted in 10 different fields ($p<.0003$).

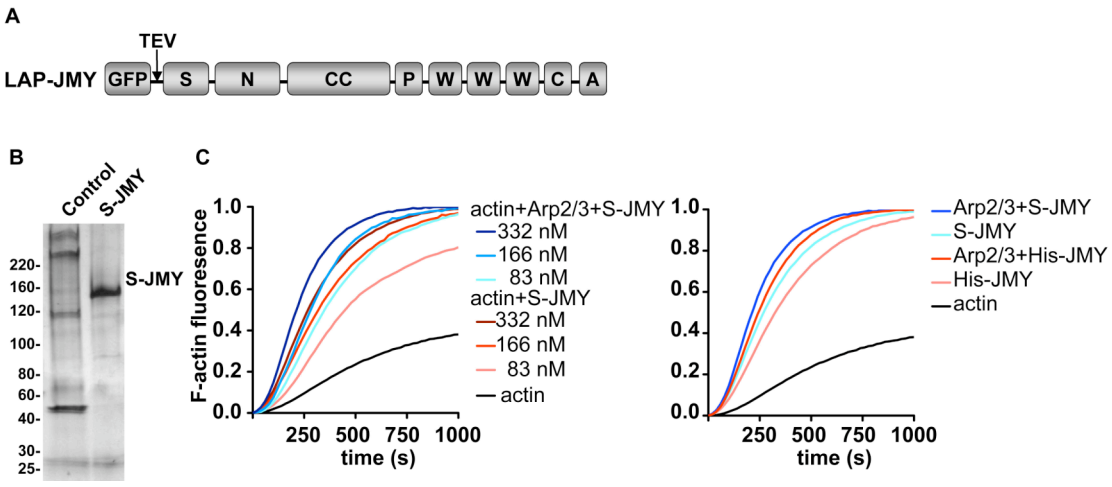

Figure 3.2: JMY expressed in mammalian cells is an actin nucleator and nucleation promoting factor *in vitro*.

(A) Domain organization of LAP-JMY, which consists an N-terminal GFP, TEV protease cleavage site and S peptide tag.

(B) 293 cells or stably-transfected 293 cells that express LAP-JMY were subjected to LAP-based affinity purification, and purified proteins were resolved by SDS-PAGE and stained with silver stain.

(C) Actin (2μm, 7% pyrene-labeled) was polymerized with the indicated concentrations of S-JMY from mammalian cells or His-JMY from insect cells with or without 20 nM Arp2/3 complex. When not indicated, 332 nM LAP-JMY and His-JMY was used.

active, and is not autoinhibited like the NPFs N-WASP and WASP (Kim et al., 2000; Miki et al., 1998; Prehoda et al., 2000; Tomasevic et al., 2007).

JMY-WWWCA promotes actin-based motility by an Arp2/3 complex-dependent mechanism

To examine the relative contributions of JMY's intrinsic nucleating activity and its Arp2/3 complex stimulating activity to actin assembly in cell cytosol, we next examined the ability of JMY-WWWCA to promote actin-based bead motility in *Xenopus laevis* egg extracts. In similar experiments, other NPFs promote bead motility by an Arp2/3 complex-dependent mechanism (Yarar et al., 2002). When 0.5 μm-diameter beads were coated with JMY-WWWCA and added to cell extracts, they underwent actin-based motility and formed comet tails similar to those induced by other NPFs (Figure 3A, C) (Cameron et al., 1999; Jeng et al., 2004; Yarar et al., 2002; Yarar et al., 1999). In contrast, beads coated with the Arp2/3-activation defective mutant JMY-WWWCA (W981A) did not undergo motility or form comet tails (Figure 3B). Together these results demonstrate that JMY-WWWCA is sufficient to direct actin-based motility in cell cytosol, and that motility requires its ability to activate the Arp2/3 complex.

JMY is widely expressed in mammalian tissues and cell lines

To investigate the expression pattern of JMY in mammalian tissues and cell lines, we generated a polyclonal antibody against full-length His-JMY. The affinity-purified antibody recognized a major protein of approximately 125 kDa, corresponding to JMY, in extracts from a wide range of mouse tissues (Figure 3A) and mammalian cell lines (Figure 3B). JMY was expressed in most tissues examined, and exhibited particularly high expression levels in brain and testis. In addition, JMY was expressed in all cultured mammalian cell lines that we tested, including monkey Cos7 and human HFF fibroblasts, human 293 epithelial cells, human SY5Y, mouse Neuro 2a and rat PC-12 neuronal cells (Figure 3B). Taken together, these results suggest that JMY has a wide expression profile in mammalian tissues and cell lines.

JMY localizes to both nucleus and cytosol

To begin to investigate the cellular function of JMY, we examined its localization in cells. Given that JMY has been reported to localize to both the nucleus and cytosol or leading edge (Coutts et al., 2007; Coutts et al., 2009; Zuchero et al., 2009), we first assessed its relative distribution between these two compartments by biochemical fractionation of monkey Cos7 and human 293 cell lysates into nuclear and cytosolic fractions. In these experiments, the nuclear marker protein NonO and the cytosolic marker protein tubulin fractionated with their respective compartments with little cross-contamination, confirming the fidelity of the procedure (Figure 5A and B). In each cell line, endogeous JMY was

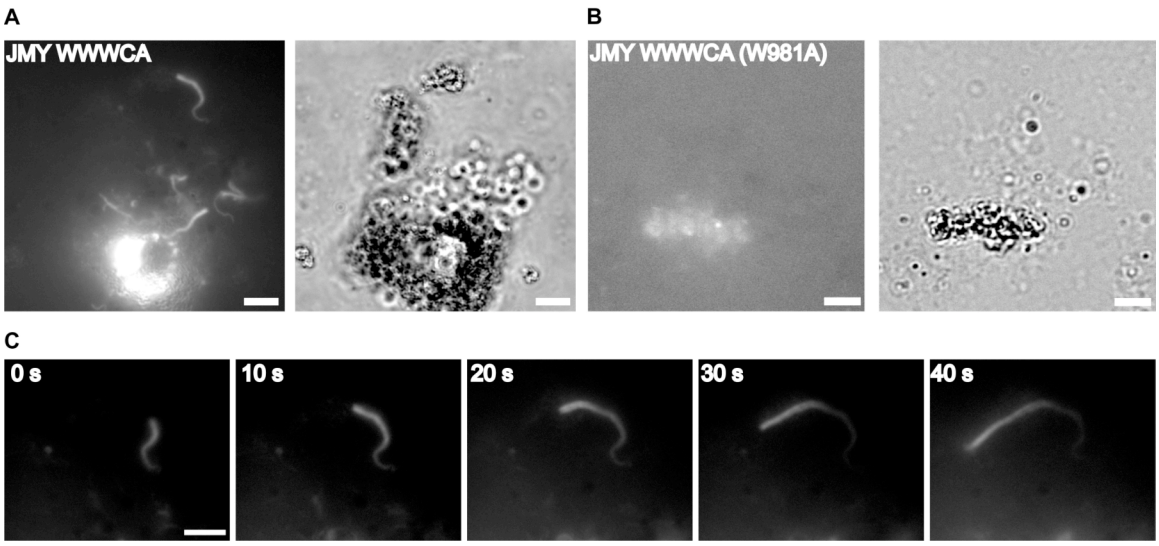

Figure 3.3: JMY-WWWCA-coated beads undergo actin-based motility in *Xenopus laevis* extracts

(A and B) JMY-WWWCA- and JMY-WWWCA (W981A)-coated beads were incubated in *X. laevis* egg extracts supplemented with rhodamine-actin, and actin structures were visualized by fluorescence and phase-contrast microscopy. Scale bar 2.5 μm.

(C) Time-lapse images of a rhodamine-labeled actin comet tail trailing behind a moving JMY-WWWCA bead. Images were taken at 10 s intervals. Scale bar 2.5 μm.

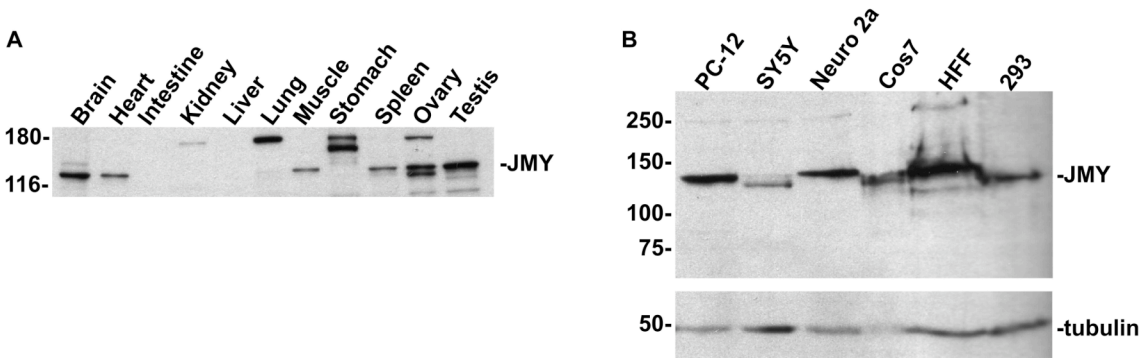

Figure 3.4: JMY is widely expressed in mammalian tissues and cell lines.

(A) Extracts from mouse tissues (20 μg/lane) or **(B)** from Neuro-2a, SY5Y, PC-12, HFF, Cos7 and 293 cells were immunoblotted with anti-JMY antibody. Anti-tubulin antibody was used as a loading control.

found in both cytosolic and nuclear fractions, but was highly enriched in the cytosol (Figure 5A and 5B). Given the function of JMY as a transcriptional co-activator in the nucleus (Coutts et al., 2007; Coutts et al., 2009; Shikama et al., 1999), this observation might imply that actin-dependent functions of JMY exist in the cytosol. Further fractionation of the cytosolic extracts into membrane-associated and soluble components demonstrated that JMY did not associate with membranes (data not shown), in contrast to other class I NPFs including WHAMM, the closest vertebrate homologue of JMY in sequence (Campellone et al., 2008).

To further assess the subcellular localization of JMY, we transfected Cos7 and U2OS cells with an N-terminally EGFP-tagged variant of JMY (GFP-JMY) and observed its intracellular distribution. Consistent with the results of fractionation studies, GFP-JMY localized to both the nucleus and cytosol (Figure 5C and 5D). Interestingly, the localization pattern was heterogeneous, with some cells showing more prominent GFP-JMY fluorescence in the nucleus and others showing more in the cytosol with enrichment in the perinuclear area (Figure 5C and 5D). In some instances, GFP-JMY appeared to be concentrated with actin filaments at the cell periphery in membrane ruffles, similar to what has been reported for endogenous JMY at the leading edge of mouse melonama and human neutrophil cells (Zuchero et al., 2009). Our results indicate that the localization pattern of JMY differs for individual cells, suggesting that it is subject to regulation based on the physiological state of the cell.

Full-length JMY is less active than JMY-WWWCA in promoting ectopic actin assembly in cells

To further investigate the function and regulation of JMY in actin assembly in cells, we assessed the effect of GFP-JMY expression on F-actin abundance and organization. In a subpopulation of U2OS cells, overexpression of GFP-JMY resulted in the formation of ectopic F-actin clusters that co-localize with GFP-JMY (Figure 6A), similar to previous observations (Coutts et al., 2009; Zuchero et al., 2009). In addition, Neuro 2a cells that were transfected with mCherry-JMY and then induced for neuronal differentiation by retinoic acid treatment, resulted in accumulation of F-actin in the perinuclear region of transfected cells (Figure 6B). These observations indicate that overexpression of JMY can result in actin assembly in a subset of cells.

For other NPFs, the effect of protein overexpression on the overall quantity of F-actin in cells is correlated with their mode of regulation. For WASP and N-WASP, which are regulated by autoinhibition (Kim et al., 2000; Miki et al., 1998; Prehoda et al., 2000), overexpression of the full-length protein does not lead to an overall increase in cellular F-actin (Campellone et al., 2008). In contrast, for WAVEs, which are regulated by trans-inhibition (Derivery et al., 2009; Eden et al., 2002; Ismail et al., 2009; Lebensohn and Kirschner, 2009), overexpression of the full-length protein leads to a global increase in cellular F-actin(Campellone et al., 2008). To begin to address whether JMY may be regulated by autoinhibition or trans regulation, we compared the effects of expressing full-length GFP-JMY

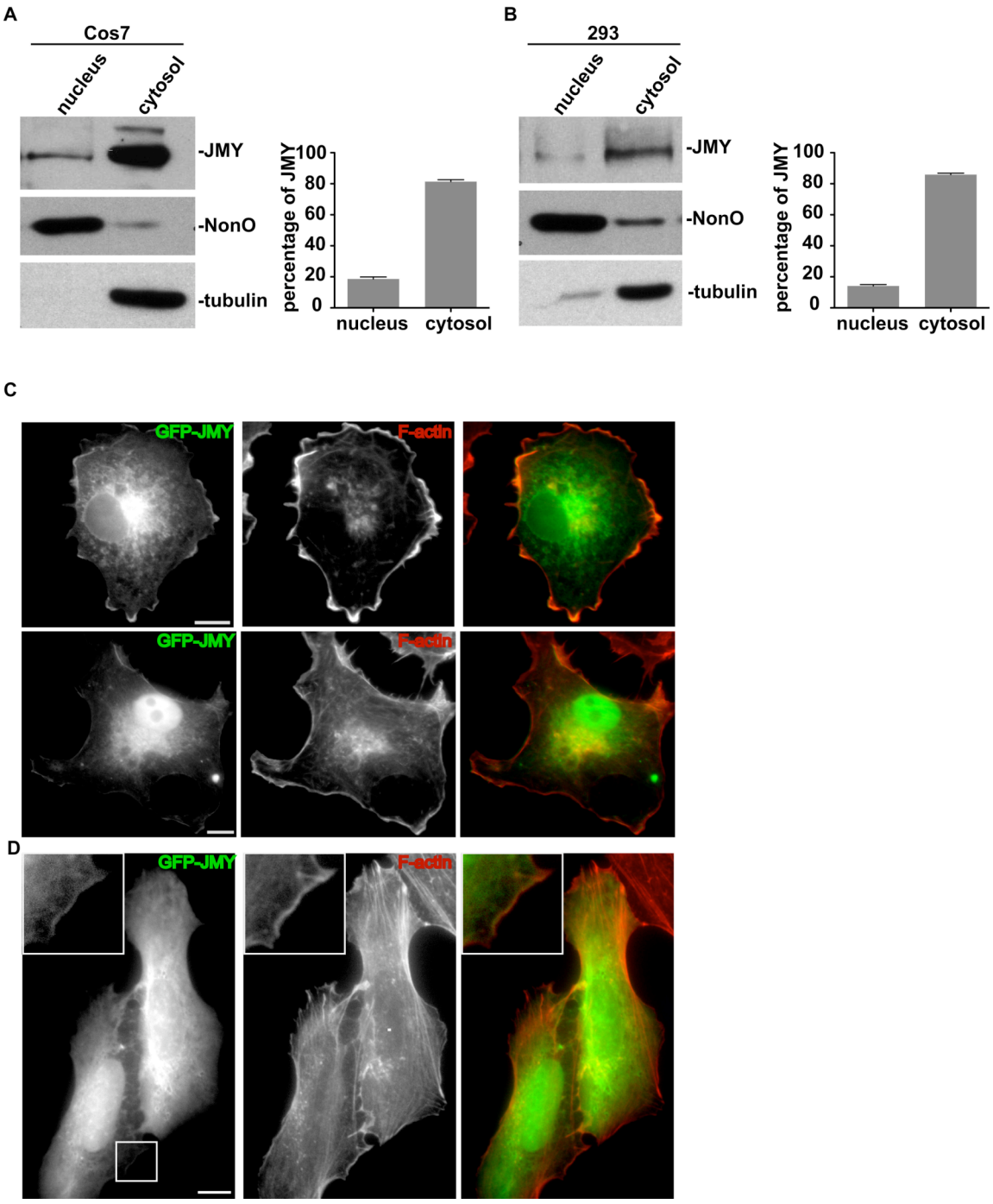

Figure 3.5: JMY localizes to both the nucleus and the cytosol.

(A and B) Immunoblots of nuclear and cytoplasmic fractions from **(A)** Cos7 or **(B)** 293 cells. 30 μg each of nuclear and cytosolic fractions were resolved by SDS-PAGE and immunoblotted with antibodies to JMY, NonO (a nuclear marker) and tubulin (a cytosolic marker). Relative amounts of JMY in the nucleus and cytosol

were determined by densitometry and are represented as the mean ± SEM of three experiments.

(C and D) Images of GFP-JMY in **(C)** Cos7 and **(D)** U2OS cells stained for actin filaments with Alexa-568 phalloidin. JMY localizes to both the nucleus and the cytosol, and is sometimes enriched in membrane ruffles (5A upper panel, 5D inset). Scale bar 5 μm.

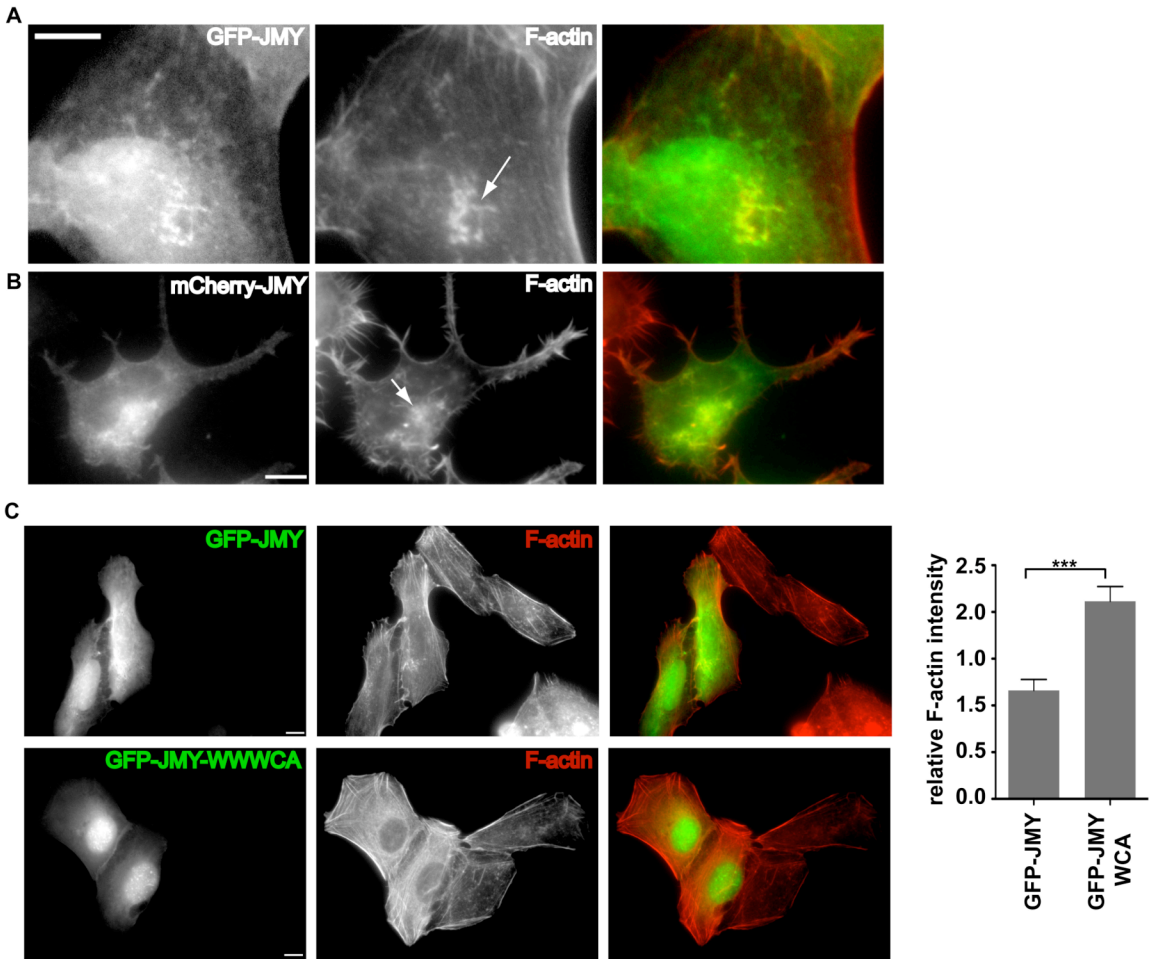

Figure 3.6: JMY expression induces formation of F-actin clusters but does not cause global increase cellular F-actin content

(A) GFP-JMY (green on right) and F-actin (red on right, stained with Alexa-568 phalloidin) in transfected U2OS cells. Arrows show F-actin clusters**.** Scale bar 5 μm.

(B) mCherry-JMY (green on right) and F-actin (red on right, stained with Alexa-488 phalloidin) in transfected Neuro 2a cells. Arrows show F-actin clusters**.** Scale bar 5 μm.

(C) (Top) GFP-JMY (green on right) and F-actin (red on right, stained with Alexa-568 phalloidin) in transfected and non-transfected U2OS cells. (Bottom) GFP-JMY-WWWCA (green on right) and F-actin (red on right) in transfected and non-transfected U2OS cells. Scale bars 5 μm.

(D) Quantification of the ratio of F-actin staining intensity in transfected/non-transfected U2OS cells shown in (C). Data are the mean ± SEM of three different experiments with 25 cells examined per sample ($p<.0003$).

or truncated JMY-WWWCA on F-actin content by quantifying the ratio of fluorescent phalloidin staining intensity in transfected compared with nearby non-transfected cells. Cells transfected with GFP-JMY-WWWCA had a significant increase in F-actin content relative to non-transfected cells (mean ± SEM ratio transfected/non-tranfected of 2.12 ± 0.15). However, cells tranfected with GFP-JMY were indistinguishable from nearby untransfected controls (mean ratio 1.16±0.11) (Figure 6C). The observation that JMY-WWWCA expression increases the F-content of cells whereas full length GFP-JMY does not suggests that full-length JMY is somehow inhibited for its ability to polymerize actin in cells.

JMY does not play a crucial role in the migration of mouse embryonic fibroblast cells

Previous studies have suggested that JMY plays a role in cell migration in U2OS cells (Coutts et al., 2009; Zuchero et al., 2009). To investigate this potential function in other cell types, we examined the effect of silencing JMY by RNAi. Mouse embryonic fibroblasts (MEFs) were transfected with control GAPDH siRNA or JMY siRNA, and depletion of JMY was confirmed by immunoblotting (Figure 7A). To measure cell migration, confluent cell monolayers were scratch-wounded and the percentage of wound closure was monitored over 4.5 h by phase contrast microscopy. JMY-silenced cells and control cells (%81.81±4.5) had a statistically similar percentage of wound closure after 4.5 h (Figure 7B-D; mean ± SEM of 76% ± 5% closure for JMY silenced cells, 82% ± 5% for controls, p=0.45**)**. Previous studies have shown that the NPF WAVE2 localizes to lamellipodia and is crucial for cell motility (Suetsugu et al., 2003; Yamazaki et al., 2003; Yan et al., 2003), raising the possibility that the failure to observe a defect in JMY-silenced cells might be due to functional redundancy between JMY and WAVE2. To test this, we performed a similar wound healing assays in matched WAVE2$^{-/-}$ MEF cells (Yan et al., 2003) also silenced for JMY expression as described above (Figure 6A). Although WAVE2$^{-/-}$ cells were defective in wound closure compared to WAVE$^{+/+}$ controls, further silencing of JMY expression did not cause a more pronounced migration defect (Figure 7C, D; 53% ± 4% closure for WAVE2$^{-/-}$ versus 51% ± 3% for WAVE2$^{-/-}$ and JMY silenced, p=0.68). Thus, we were unable to detect a role for JMY in cell motility in MEF cells.

JMY inhibits neurite outgrowth upon differentiation of neuronal cells

Because JMY is highly expressed in brain relative to other tissues, we hypothesized that it might have a tissue-specific function in neuronal cells. One well studied *in vitro* model system for neuritogenesis and neuronal differentiation are mouse neuroblastoma Neuro2a cells (Wu et al., 1998), which can be induced to differentiate by retinoic acid (RA) treatment. To address the role of JMY in neuritogenesis and neuronal differentiation, we first perfomed a time-course experiment to determine whether JMY protein levels changed during retinoic acid (RA)-induced differentiation. Interestingly, we observed a

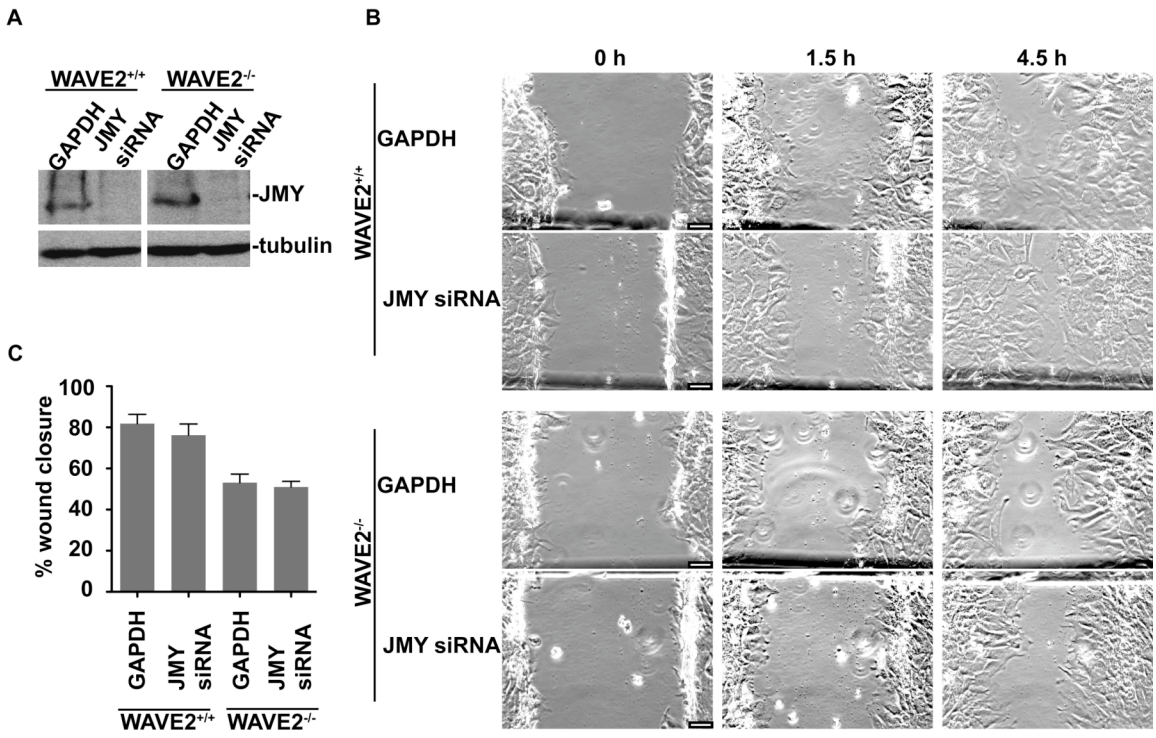

Figure 3.7: JMY depletion does not affect cell migration in mouse embryonic fibroblasts

(A) Extracts from WAVE2$^{+/+}$ and WAVE2$^{-/-}$ cells transfected with GAPDH or JMY siRNAs for 72 h were resolved by SDS-PAGE and immunoblotted with anti-JMY and anti-tubulin antibodies.

(B) Timecourse (0 – 4.5 h) of wound closure in WAVE2$^{+/+}$ and WAVE2$^{-/-}$ cells 72 h after transfection with either GAPDH or JMY siRNA**.** Scale bar 10 μm.

(C) Quantification of the percentage of wound closure 4.5 h after wound initiation. Data represent the mean ± SEM of the remaining wound area of three independent experiments.

strong down regulation of JMY steady-state protein levels within 48 h of RA treatment compared to undifferentiated cells (Figure 8A, B), suggesting that JMY function might be regulated during neuronal differentiation and neurite development.

To further investigate whether JMY is functionally important for neuronal differentiation, we examined the effect of JMY silencing by RNAi on RA-induced differentiation, neurite outgrowth and neuronal morphogenesis. Neuro 2a cells were transfected with control GAPDH or two independent JMY siRNAs, and induced to differentiate by RA treatment. Depletion of JMY was confirmed by immunoblotting (Figure 8C). We first investigated the ability of cells to form neurites upon JMY depletion. Surprisingly, we observed a significant increase in the number of cells bearing neurites in JMY silenced cells (Figure 8D, F; 28% ± 2% for JMY siRNA#1 and 31% ± 3% for JMY siRNA#2 versus 15% ± 1 for control cells). The fact that two independent JMY siRNAs caused similar effects on neurite outgrowth confirms that the pheynotype is specific to JMY silencing.

We next investigated the effect of JMY depletion on neuronal morphogenesis by quantifying a variety of neurite characteristics including mean neurite length, mean number of neurites per cell, and mean number of neurite branchpoints per unit neurite length (Figure 8E). However, we did not observe a significant effect of JMY silencing on any of these parameters. Thus the function of JMY may be restricted to the early stages of neuritogenesis.

Discussion

JMY was recently discovered as a unique actin assembly protein, that nucleates actin as both a tandem monomer binding nucleator and an NPF (Zuchero et al., 2009) and also functions as a p300 coactivator in the p53 response (Coutts et al., 2009; Shikama et al., 1999). Here we show that full-length JMY differs in its ability to polymerize actin *in vitro* and in cells. Although JMY and its truncated WWWCA domain have similar actin nucleating and Arp2/3-complex activating activities *in vitro*, the ability of full-length JMY to polymerize actin is somewhat inhibited in cells, suggesting potential mechanisms for JMY regulation. We also uncover a new function for JMY in neuronal outgrowth and differentiation.

Our results demonstrate that full-length JMY is a potent actin nucleator and Arp2/3-activating NPF and has comparable actin polymerization activity levels to its WWWCA domain *in vitro*. Recombinant JMY purified from a stably transfected mammalian cell line also had comparable activity to JMY purified from insect cells and did not co-purify with any stoichiometric binding partners. In addition, JMY did not fractionate with high molecular weight complexes in brain extracts (data not shown) as do the WAVEs (Eden et al. 2002). These findings do not support a model in which JMY is trans-regulated by binding partners in a protein complex, although they do not completely rule out this possibility. Whereas WASP/N-WASP and the WAVEs are regulated by different mechanisms, the full-length recombinant proteins were reported to be either

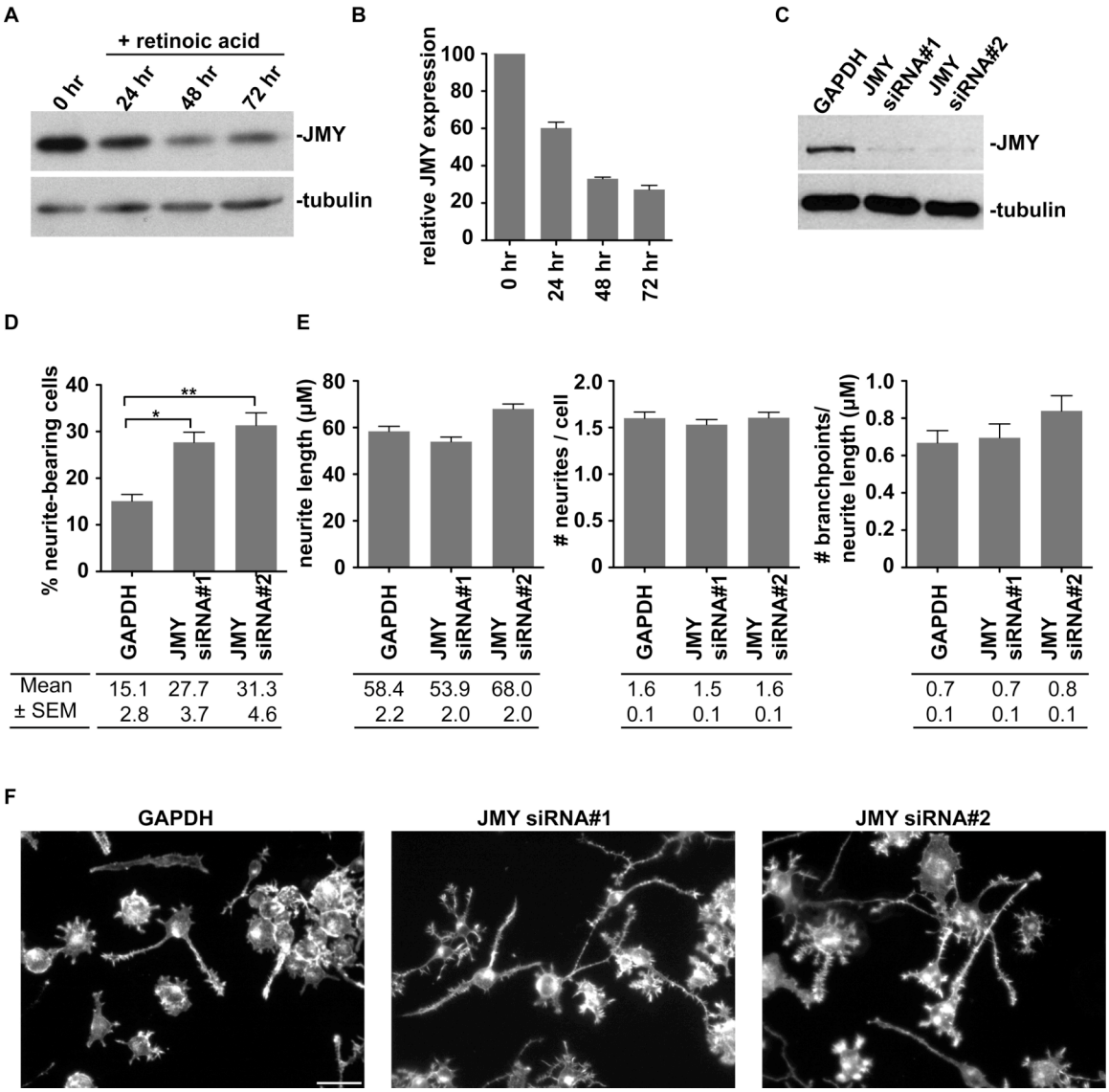

Figure 3.8: JMY inhibits neurite outgrowth in Neuro 2a cells

(A) Extracts from Neuro 2a cells that were induced for differentiation with retinoic acid for the indicated timepoints were resolved by SDS-PAGE and blotted with anti-JMY antibodies and with anti-tubulin antibodies as a loading control.

(B) Quantification of JMY expression levels relative to tubulin by densitometry. Data are the mean ± SEM of two experiments.

(C) Extracts from Neuro 2a cells treated with control GAPDH siRNA or each of two independent JMY siRNAs for 96 h were resolved by SDS-PAGE and immunoblotted with anti-JMY antibodies and anti-tubulin antibodies.

(D) Quantification of percentage of cells bearing neurites in Neuro 2a cells transfected with control GAPDH siRNA and two independent JMY siRNAs.

Data are the mean ± SEM of three experiments with 500 cells quantified for each ($p<.002$).

(E) Quantification of neurite length, number of neurites/cell and number of branchpoints/neurite length in control versus JMY-silenced Neuro 2a cells. Data are the mean ± SEM of two experiments with 100 cells quantified for each.

(F) F-actin (stained with Alexa 488-phalloidin) in control and JMY-silenced Neuro 2a cells. Scale bar 10 μm.

active (Innocenti et al., 2004; Rohatgi et al., 1999; Yarar et al., 1999) or inactive (Derivery et al., 2009; Ismail et al., 2009; Lebensohn and Kirschner, 2009; Tomasevic et al., 2007) *in vitro* depending on the cell type selected for expression and the experimental conditions used for purification and reconstitution. Therefore, the *in vitro* actin assembly data for full-length recombinant JMY is not sufficient to derive conclusions on the mode of its regulation.

When expressed in cells, JMY induced the formation of F-actin structures that co-localized with JMY, suggesting that it can induce actin polymerization in cells, similar to its *in vitro* activity. However, cells expressing intermediate to high levels of full-length JMY did not have a significant increase in their overall F-actin content as compared with cells expressing the truncated JMY-WWWCA, implying that full-length JMY is somewhat inhibited for its ability to polymerize actin relative to the WWWCA domain. Similarly, cells expressing full-length N-WASP did not exhibit an increase in the F-actin content of cells (Campellone et al., 2008), suggesting that JMY might be regulated by autoinhibition like WASP/N-WASP. In contrast to JMY and N-WASP, cells expressing full-length WAVE2 exhibited a significant increase in their F-actin content (Campellone et al., 2008). Based on this observation and our data on the lack of interacting partners of JMY and its size based on sucrose gradient sedimentation, trans-regulation of JMY by interacting partners is unlikely. In addition to autoinhibition, regulation of JMY by other mechanisms such as posttranslational modifications is also possible, as is the case for WASP (Cory et al., 2003; Torres and Rosen, 2003) and WAVE1 (Kim et al., 2006), which require phosphorylation for activation and WAVE2, which requires phosphorylation and binding to Rac-GTP and acidic phospholipids for activation (Lebensohn and Kirschner, 2009). Further investigation of autoinhibition and posttranslational modifications as possible regulatory mechanisms of JMY is required.

In contrast to previous studies that identified the nucleus as the primary site of JMY localization (Zuchero et al., 2009), the results of our cell fractionation studies show that its primary localization is in the cytosol. Interestingly, in some cells JMY localizes more extensively in the nucleus and in others more extensively in the cytosol, suggesting that JMY shuttles in and out of nucleus depending on the physiological state of the cell. Although previous studies demonstrated that JMY is transported into the nucleus upon DNA damage (Coutts et al., 2007; Coutts et al., 2009) and relocates from the nucleus to the leading edge in migrating cells (Zuchero et al., 2009), neither of these triggers was activated in the conditions we used for fractionation and localization experiments. Future work is required to determine the mechanisms that regulate the nuclear/cytoplasmic distribution of JMY and the upstream signaling pathways that regulate this process.

The cytosolic pool of JMY did not localize to specific cellular structures, other than a small proportion that co-localized with actin in membrane ruffles. Despite its localization to membrane ruffles, we did not observe any defect in cellular motility in JMY-depleted MEF cells, even when JMY was depleted in cells lacking WAVE2. This observation is in disagreement with recent studies that showed that JMY functions in cellular motility by activating Arp2/3-mediated actin polymerization (Zuchero et al., 2009) and down-regulating

cadherin expression (Coutts et al., 2009). It is noteworthy that we used mouse embryonic fibroblasts to examine the function of JMY in wound healing assays, whereas other groups used U2OS epithelial cells. Therefore, it is possible that differences in cell type might have contributed to any apparent discrepancies.

In addition to examining its role in migration, we also tested the function of JMY in neurons, because it is highly expressed in brain relative to other tissues. The actin cytoskeleton plays important roles in various stages of neuronal development, including neurite outgrowth and differentiation, axon pathfinding and dendritic spine formation and maintenance (Kessels et al., 2010). Although the molecular machinery that regulates the reorganization of the actin cytoskeleton in neurons is not fully characterized, different actin nucleators including the Arp2/3 complex (Korobova and Svitkina, 2008) and its NPFs N-WASP (Banzai et al., 2000; Pinyol et al., 2007) and WAVE1 (Kim et al., 2006) and also tandem actin-monomer-binding nucleator Cordon-bleu (Ahuja et al., 2007) were shown to positively regulate some of these stages of neuronal development through their role in growth cone formation and dynamics. In contrast, we found that JMY depletion in neuronal cells resulted in a significant increase in the number of cells that formed neurites, suggesting that JMY might be a negative regulator of neurite outgrowth. Our observation of significant down-regulation of steady state JMY protein levels upon differentiation further supports this inhibitory function. One key future challenge is to understand the molecular mechanism of the inhibitory role of JMY in neurite outgrowth.

Given the dual function of JMY as a transcription co-activator and actin assembly protein, there are two possible mechanisms through which it might inhibit neurite outgrowth. One possible mechanism is via a role for JMY in regulating actin polymerization and dynamics in neurons. Small Rho GTPases including Rac, Rho and Cdc42 have been shown to be important for cytoskeletal dynamics in neurons (Govek et al., 2005), and it is possible that JMY might be one of the downstream effectors of the Rho GTPases. Rac and Cdc42 function in lamellipodia and filopodia formation in the growth cone (Kozma et al., 1997), thus promoting neurite formation. On the other hand, activation of Rho inhibits neurite formation and induces retraction by antagonizing Rac activity and promoting the formation of thick ring-like cortical actin filaments at the cell periphery that increase the cytoskeletal tension for neurite outgrowth (Yamaguchi et al., 2001). Considering the inhibitory effect of JMY on neurite formation, we propose that JMY may be an effector protein for Rho that functions in the assembly of the cortical actin cytoskeleton at the cell periphery of neurons. The observations that inactivation of Rho activity by its inhibitors (Jalink et al., 1994) or expression of dominant negative Rho (Sebok et al., 1999) induced neurite formation in rat adrenal medulla PC12 and mouse neuroblastoma N1E-115 cells, similar to depletion of JMY, is consistent with this hypothesis. A balance between the antagonistic activities of different Rho GTPases was suggested to regulate neuritogenesis, and it is possible that JMY participates in establishing this balance. Future work will be aimed at testing this hypothesis.

A second mechanism for JMY inhibition of neurite outgrowth may be via a role as a transcriptional regulator during RA-induced differentiation of

neuronal cells. Retinoic acid serves as a master regulator of gene expression during neuronal differentiation by binding to nuclear RA receptors and modulating expression of genes that participate in neuronal differentiation including neutrotrophin receptors and other signaling molecules (Clagett-Dame et al., 2006). Because JMY functions in transcriptional regulation by binding to p300 (Shikama et al., 1999), a transcriptional co-activator of diverse transcription factors, it might exert its inhibitory function by modulating RA-mediated gene expression. Future work is required to distinguish between the functions of JMY as a transcription cofactor or actin assembly protein in neurons.

Although our study sheds light on the cellular regulation and function of JMY, numerous questions remain. One question concerns the nature of JMY regulation in cells. Future work is required to determine the upstream signaling pathways that regulate the activity of JMY and control its transport between the nucleus and cytosol. Different actin assembly proteins are regulated by small GTPases and posttranslational modifications and it is likely that JMY is also regulated by similar mechanisms. A second question concerns the biological significance of why JMY combines two very different cellular functions, transcriptional regulation and actin assembly, in one protein. It will be important to examine transcriptional and actin-related functions of JMY in cellular processes including neuritogenesis to understand whether they work together or independently in cells. Furthermore, given the function of nuclear actin in transcription, it is tempting to speculate that JMY is a molecular link between the actin cytoskeleton and transcription in the nucleus. Further investigation of these questions will contribute to our understanding of the regulation and dynamics of the actin cytoskeleton in cells.

References

Abramoff, M.D., Magelhaes, P.J., Ram, S.J. (2004). Image porcessing with ImageJ. Biophotonics International 11, 36-42.

Ahuja, R., Pinyol, R., Reichenbach, N., Custer, L., Klingensmith, J., Kessels, M.M., and Qualmann, B. (2007). Cordon-bleu is an actin nucleation factor and controls neuronal morphology. Cell *131*, 337-350.

Banzai, Y., Miki, H., Yamaguchi, H., and Takenawa, T. (2000). Essential role of neural Wiskott-Aldrich syndrome protein in neurite extension in PC12 cells and rat hippocampal primary culture cells. J Biol Chem *275*, 11987-11992.

Cameron, L.A., Footer, M.J., van Oudenaarden, A., and Theriot, J.A. (1999). Motility of ActA protein-coated microspheres driven by actin polymerization. Proc Natl Acad Sci U S A *96*, 4908-4913.

Campellone, K.G., Webb, N.J., Znameroski, E.A., and Welch, M.D. (2008). WHAMM is an Arp2/3 complex activator that binds microtubules and functions in ER to Golgi transport. Cell *134*, 148-161.

Campellone, K.G., and Welch, M.D. (2010). A nucleator arms race: cellular control of actin assembly. Nat Rev Mol Cell Biol *11*, 237-251.

Cheeseman, I.M., and Desai, A. (2005). A combined approach for the localization and tandem affinity purification of protein complexes from metazoans. Sci STKE *2005*, pl1.

Clagett-Dame, M., McNeill, E.M., and Muley, P.D. (2006). Role of all-trans retinoic acid in neurite outgrowth and axonal elongation. J Neurobiol *66*, 739-756.

Cory, G.O., Cramer, R., Blanchoin, L., and Ridley, A.J. (2003). Phosphorylation of the WASP-VCA domain increases its affinity for the Arp2/3 complex and enhances actin polymerization by WASP. Mol Cell *11*, 1229-1239.

Coutts, A.S., Boulahbel, H., Graham, A., and La Thangue, N.B. (2007). Mdm2 targets the p53 transcription cofactor JMY for degradation. EMBO Rep *8*, 84-90.

Coutts, A.S., Weston, L., and La Thangue, N.B. (2009). A transcription co-factor integrates cell adhesion and motility with the p53 response. Proc Natl Acad Sci U S A *106*, 19872-19877.

Derivery, E., Lombard, B., Loew, D., and Gautreau, A. (2009). The Wave complex is intrinsically inactive. Cell Motil Cytoskeleton *66*, 777-790.

Edelstein, A., Amodaj, N., Hoover, K., Vale, R., and Stuurman, N. (2010). Computer control of microscopes using microManager. Curr Protoc Mol Biol *Chapter 14*, Unit14 20.

Eden, S., Rohatgi, R., Podtelejnikov, A.V., Mann, M., and Kirschner, M.W. (2002). Mechanism of regulation of WAVE1-induced actin nucleation by Rac1 and Nck. Nature *418*, 790-793.

Firat-Karalar, E.N., and Welch, M.D. (2010). New mechanisms and functions of actin nucleation. Curr Opin Cell Biol.

Goley, E.D., Rodenbusch, S.E., Martin, A.C., and Welch, M.D. (2004). Critical conformational changes in the Arp2/3 complex are induced by nucleotide and nucleation promoting factor. Mol Cell *16*, 269-279.

Govek, E.E., Newey, S.E., and Van Aelst, L. (2005). The role of the Rho GTPases in neuronal development. Genes Dev *19*, 1-49.

Innocenti, M., Zucconi, A., Disanza, A., Frittoli, E., Areces, L.B., Steffen, A., Stradal, T.E., Di Fiore, P.P., Carlier, M.F., and Scita, G. (2004). Abi1 is essential for the formation and activation of a WAVE2 signalling complex. Nat Cell Biol *6*, 319-327.

Ismail, A.M., Padrick, S.B., Chen, B., Umetani, J., and Rosen, M.K. (2009). The WAVE regulatory complex is inhibited. Nat Struct Mol Biol *16*, 561-563.

Jalink, K., van Corven, E.J., Hengeveld, T., Morii, N., Narumiya, S., and Moolenaar, W.H. (1994). Inhibition of lysophosphatidate- and thrombin-induced neurite retraction and neuronal cell rounding by ADP ribosylation of the small GTP-binding protein Rho. J Cell Biol *126*, 801-810.

Jeng, R.L., Goley, E.D., D'Alessio, J.A., Chaga, O.Y., Svitkina, T.M., Borisy, G.G., Heinzen, R.A., and Welch, M.D. (2004). A Rickettsia WASP-like protein activates the Arp2/3 complex and mediates actin-based motility. Cell Microbiol *6*, 761-769.

Kessels, M.M., Schwintzer, L., Schlobinski, D., and Qualmann, B. (2010). Controlling actin cytoskeletal organization and dynamics during neuronal morphogenesis. Eur J Cell Biol.

Kim, A.S., Kakalis, L.T., Abdul-Manan, N., Liu, G.A., and Rosen, M.K. (2000). Autoinhibition and activation mechanisms of the Wiskott-Aldrich syndrome protein. Nature *404*, 151-158.

Kim, Y., Sung, J.Y., Ceglia, I., Lee, K.W., Ahn, J.H., Halford, J.M., Kim, A.M., Kwak, S.P., Park, J.B., Ho Ryu, S., *et al.* (2006). Phosphorylation of WAVE1 regulates actin polymerization and dendritic spine morphology. Nature *442*, 814-817.

Korobova, F., and Svitkina, T. (2008). Arp2/3 complex is important for filopodia formation, growth cone motility, and neuritogenesis in neuronal cells. Mol Biol Cell *19*, 1561-1574.

Kozma, R., Sarner, S., Ahmed, S., and Lim, L. (1997). Rho family GTPases and neuronal growth cone remodelling: relationship between increased complexity induced by Cdc42Hs, Rac1, and acetylcholine and collapse induced by RhoA and lysophosphatidic acid. Mol Cell Biol *17*, 1201-1211.

Lanzetti, L. (2007). Actin in membrane trafficking. Curr Opin Cell Biol *19*, 453-458.

Lebensohn, A.M., and Kirschner, M.W. (2009). Activation of the WAVE complex by coincident signals controls actin assembly. Mol Cell *36*, 512-524.

Marchand, J.B., Kaiser, D.A., Pollard, T.D., and Higgs, H.N. (2001). Interaction of WASP/Scar proteins with actin and vertebrate Arp2/3 complex. Nat Cell Biol *3*, 76-82.

Maresca, T.J., and Heald, R. (2006). Methods for studying spindle assembly and chromosome condensation in Xenopus egg extracts. Methods Mol Biol *322*, 459-474.

Miki, H., Sasaki, T., Takai, Y., and Takenawa, T. (1998). Induction of filopodium formation by a WASP-related actin-depolymerizing protein N-WASP. Nature *391*, 93-96.

Pinyol, R., Haeckel, A., Ritter, A., Qualmann, B., and Kessels, M.M. (2007). Regulation of N-WASP and the Arp2/3 complex by Abp1 controls neuronal morphology. PLoS One *2*, e400.

Pollard, T.D., and Cooper, J.A. (2009). Actin, a central player in cell shape and movement. Science *326*, 1208-1212.

Prehoda, K.E., Scott, J.A., Mullins, R.D., and Lim, W.A. (2000). Integration of multiple signals through cooperative regulation of the N-WASP-Arp2/3 complex. Science *290*, 801-806.

Rohatgi, R., Ma, L., Miki, H., Lopez, M., Kirchhausen, T., Takenawa, T., and Kirschner, M.W. (1999). The interaction between N-WASP and the Arp2/3 complex links Cdc42-dependent signals to actin assembly. Cell *97*, 221-231.

Sebok, A., Nusser, N., Debreceni, B., Guo, Z., Santos, M.F., Szeberenyi, J., and Tigyi, G. (1999). Different roles for RhoA during neurite initiation, elongation, and regeneration in PC12 cells. J Neurochem *73*, 949-960.

Shikama, N., Lee, C.W., France, S., Delavaine, L., Lyon, J., Krstic-Demonacos, M., and La Thangue, N.B. (1999). A novel cofactor for p300 that regulates the p53 response. Mol Cell *4*, 365-376.

Suetsugu, S., Yamazaki, D., Kurisu, S., and Takenawa, T. (2003). Differential roles of WAVE1 and WAVE2 in dorsal and peripheral ruffle formation for fibroblast cell migration. Dev Cell *5*, 595-609.

Tomasevic, N., Jia, Z., Russell, A., Fujii, T., Hartman, J.J., Clancy, S., Wang, M., Beraud, C., Wood, K.W., and Sakowicz, R. (2007). Differential regulation of WASP and N-WASP by Cdc42, Rac1, Nck, and PI(4,5)P2. Biochemistry *46*, 3494-3502.

Torres, E., and Rosen, M.K. (2003). Contingent phosphorylation/dephosphorylation provides a mechanism of molecular memory in WASP. Mol Cell *11*, 1215-1227.

Wu, G., Fang, Y., Lu, Z.H., and Ledeen, R.W. (1998). Induction of axon-like and dendrite-like processes in neuroblastoma cells. J Neurocytol *27*, 1-14.

Yamaguchi, Y., Katoh, H., Yasui, H., Mori, K., and Negishi, M. (2001). RhoA inhibits the nerve growth factor-induced Rac1 activation through Rho-associated kinase-dependent pathway. J Biol Chem *276*, 18977-18983.

Yamazaki, D., Suetsugu, S., Miki, H., Kataoka, Y., Nishikawa, S., Fujiwara, T., Yoshida, N., and Takenawa, T. (2003). WAVE2 is required for directed cell migration and cardiovascular development. Nature *424*, 452-456.

Yan, C., Martinez-Quiles, N., Eden, S., Shibata, T., Takeshima, F., Shinkura, R., Fujiwara, Y., Bronson, R., Snapper, S.B., Kirschner, M.W., *et al.* (2003). WAVE2 deficiency reveals distinct roles in embryogenesis and Rac-mediated actin-based motility. EMBO J *22*, 3602-3612.

Yarar, D., D'Alessio, J.A., Jeng, R.L., and Welch, M.D. (2002). Motility determinants in WASP family proteins. Mol Biol Cell *13*, 4045-4059.

Yarar, D., To, W., Abo, A., and Welch, M.D. (1999). The Wiskott-Aldrich syndrome protein directs actin-based motility by stimulating actin nucleation with the Arp2/3 complex. Curr Biol *9*, 555-558.

Zuchero, J.B., Coutts, A.S., Quinlan, M.E., Thangue, N.B., and Mullins, R.D. (2009). p53-cofactor JMY is a multifunctional actin nucleation factor. Nat Cell Biol *11*, 451-459.

CHAPTER 4

FUTURE DIRECTIONS

As described in Chapter 1, tremendous progress has been made over the course of the last decade in understanding the mechanism of actin nucleation *in vitro* and in cells. A combination of biochemical, structural and computational studies have advanced our understanding of the function of previously recognized actin nucleators and also identified new ones. Despite the wealth of information we have accumulated on the function and regulation of actin nucleators in diverse cellular processes, we are still far from understanding the complexity of cellular actin nucleation pathways. Future studies must focus on addressing the structure, function and regulation of actin nucleators and the cross-talk between them at the cellular and organismal level.

Mechanism of Arp2/3 complex activation and function by F-actin binding

Since the identification of the Arp2/3 complex as the first of the major cellular actin nucleators, we have made a lot of progress in understanding the molecular mechanism of Arp2/3 complex activity and function in actin assembly. Despite these fundamental advances, our understanding of the Arp2/3 complex activation mechanism remains incomplete. In particular, we lack information on the structural details of the Arp2/3 complex activation mechanism. As described in Chapter 2, combining computational and experimental approaches has proven useful in defining functionally important surfaces on the Arp2/3 complex required for Arp2/3-mediated activities including nucleation and Y-branching. In the future, combination of these approaches along with structural characterization of the Arp2/3 complex in various conformations will guide investigation of the different Arp2/3 complex activities in functional studies.

What are the molecular details underlying binding of the Arp2/3 complex to F-actin?

It is well established that the nucleation and Y-branching activities of the Arp2/3 complex require binding of the complex to F-actin filaments. However, the mechanism by which F-actin binding activates the Arp2/3 complex is poorly understood. In Chapter 2, we defined functionally important surface residues on ARPC2 and ARPC4 subunits required that are required for F-actin binding by experimentally testing the activity of the Arp2/3 complex mutants in activity assays. Although ARPC2/ARPC4 are thought to form the major F-actin binding interface of the Arp2/3 complex, the remaining five subunits are also predicted to bind to F-actin. To obtain a complete molecular picture of the Arp2/3 complex bound to F-actin, we need to investigate the molecular details of this interaction for the other Arp2/3 subunits using similar approaches.

The interaction between the Arp2/3 complex and F-actin was modeled using the crystal structure of the inactive complex and we designed our mutagenesis experiments based on this information. Therefore, it is possible that some of the key residues that are exposed in the active Arp2/3 complex were missed during the modeling studies. If the structure of the active Arp2/3 complex bound to its activators is determined in the future, further modeling of

the F-actin binding surface of the Arp2/3 complex using this structure will make more accurate predictions that can be tested experimentally.

Besides defining the F-actin binding surface on the Arp2/3 complex, we should also investigate how this interaction activates the complex. One possibility is that F-actin binding induces conformational changes of the Arp2/3 complex as is the case for the activation of the complex by ATP and NPFs. ATP- and NPF-induced conformational changes can be detected using a specific Arp2/3 FRET probe. Using the biochemical, structural and computational information on the Arp2/3 complex, we may be able to design similar Arp2/3 FRET probes that are sensitive to detecting F-actin induced conformational changes. If we could design such FRET probes, we could test F-actin binding mutants in FRET assays to determine the specific surfaces of the Arp2/3 complex involved in inducing the conformational changes. If F-actin binding does not activate Arp2/3 complex through conformational changes, then we should consider alternative mechanisms.

What is the in vivo significance of the binding of the Arp2/3 complex to F-actin in different cellular processes?

To investigate the functional importance of the binding of the Arp2/3 complex to F-actin in cells, we can take advantage of the F-actin binding mutants we previously generated. We can silence Arp2/3 expression in cells using RNAi, and then express wild-type Arp2/3 complex or F-actin binding mutants to assess how Arp2/3-dependent cellular processes are affected. In addition to F-actin binding mutants, future work should be aimed at defining functional surfaces of the Arp2/3 complex required for NPF binding so that we can compare the functional significance of NPF and F-actin mediated activation of the Arp2/3 complex in actin-mediated cellular processes.

Cellular regulation and function of the actin assembly protein JMY

In Chapter 3, we described the *in vitro* and *in vivo* characterization of full-length JMY with regard to its role in actin polymerization, and also discovered a previously unidentified function of JMY in neuritogenesis. Although our study sheds light on the cellular function and regulation of JMY in actin assembly, there are many unanswered questions.

What is the biological significance of JMY's combination of Arp2/3-dependent and Arp2/3-independent actin polymerization activities?

JMY is the first actin nucleator discovered that polymerizes actin both in an Arp2/3-dependent and Arp2/3-independent manner. Despite our better understanding of the molecular mechanism of JMY activity as an actin nucleator and NPF, we still don't know how JMY balances these two nucleating activities in different cellular processes. One possibility is that the two nucleating activities of JMY work together in cells. If JMY first nucleates new filaments using its intrinsic nucleation activity, and then activates the Arp2/3 complex to branch off

these filaments, this would result in a very rapid assembly of new Y-branched actin networks compared to Arp2/3 complex acting alone. An alternative explanation is that JMY polymerizes actin in different cellular contexts using only one of its nucleating abilities to generate either a Y-branched or unbranched actin network. To distinguish between these possibilities, we can use JMY mutants that are defective in Arp2/3-dependent or Arp2/3-independent nucleation in gain-of-function and loss-of-function studies of JMY in different cellular processes including neuritogenesis. In addition, we can silence Arp2/3 complex expression by RNAi and this would allow us to determine the contribution of only the intrinsic nucleation ability of JMY to the cellular process we are studying.

What is the molecular mechanism of JMY regulation in cells?

As described in Chapter 3, we propose that full-length JMY is somewhat inhibited for its ability to induce actin polymerization in cells. However, the molecular mechanism of this inhibition is still an open question. Our observations do not support either autoinhibition or trans-regulation of JMY, but one of these mechanisms is likely to be operating, and investigation of these two mechanisms is required. Determining the regulatory mechanism of JMY may be difficult, as it has been for other actin assembly proteins such as WAVE family of NPFs, resulting in controversies in the field due to differences in experimental conditions for purification and reconstitution of the complex. In addition to these two mechanisms, posttranslational modifications are another possible mechanism of JMY regulation. One approach to address these questions is the purification of the native JMY complex from tissues, particularly from brain because of the function of JMY in neuritogenesis. We can then assay the activity of the native JMY complex *in vitro* using actin polymerization assays and also analyze it by mass spectrometry to identify possible binding partners and posttranslational modifications.

JMY localizes to both nucleus and cytosol, and how it performs different functions in these compartments also hasn't been investigated. One possibility is that JMY is regulated differently in the nucleus and cytosol. We could address this possibility by purifying JMY from both nuclear and cytosolic extracts, and then comparing its interacting partners and/or posttranslational modifications to assess the similarities and differences.

How is nuclear and cytosolic transport of JMY regulated?

As described in Chapter 3, the primary localization of JMY is in the cytosol, although it is also found in the nucleus. Previous studies identified DNA damage and migratory stimuli as the two different types of triggers that shift the localization of JMY to the nucleus and cytosol, respectively. The upstream signaling pathways that regulate this nuclear and cytosolic transport require further investigation. Most other mammalian NPFs are regulated by small GTPases including Rac, Rho and Cdc42. Therefore, we speculate that JMY might also be regulated by small GTPases. To address this possibility, we can express

constitutively active or dominant negative versions of small GTPases in cells, and then determine the localization of JMY to assess any changes. We can also biochemically test this possibility by performing pull-down assays with active small GTPases to determe whether there is a direct interaction between them. These experiments should be perfomed in cells activated by different external stimuli that induce DNA damage, neuronal differentiation and cell migration to characterize the upstream signaling pathways specific to each cellular process.

How does JMY function during neuronal development and differentiation?

We described in Chapter 3 a previously unidentified function of JMY in neurite outgrowth during neuronal development and differentiation. While this finding correlates with the high expression of JMY in brain, it raises many questions regarding how JMY functions in neurons. In contrast to other actin assembly proteins that positively affect neurite initiation and extension by regulating actin polymerization and dynamics at the growth cone, our findings suggest that JMY negatively regulates neurite outgrowth. To address whether JMY exerts its function in neurons by polymerizing actin, we can try rescue experiments with full-length JMY and the actin polymerization mutant JMYΔWCA after silencing JMY expression in neurons by RNAi. If we observe rescue of the phenotype with JMY but not with JMYΔWCA, this would suggest that the actin polymerization activity of JMY is required during neurite outgrowth. To further investigate whether or not the function of JMY in neurons depends on the Arp2/3 complex, we can also try the rescue experiments with the W981A mutant of JMY that is defective in Arp2/3-mediated actin polymerization.

Alternatively, JMY might also function in neurite outgrowth by affecting the transcription of genes that are regulated upon retinoic-acid-induced differentiation of neuronal cells. To address this possibility, we can determine the expression levels of several neuronal differentiation markers upon JMY silencing or overexpression to assess whether they are affected. We could also examine the changes in the localization of JMY upon neuronal differentiation. If JMY localizes more to the nucleus upon differentiation, this would support the nuclear function of JMY as a transcription co-activator in neurons.

To examine the function of JMY in neurons, we used neuroblastoma cell lines as a model system. Although these cells are commonly used to study neuronal differentiation, not all the distinct stages of neuronal polarity and morphology establishment such as differentiation of neurites into axons and dendrites occur with high fidelity in these cell lines. To investigate the role of JMY in these later stages of neuronal differentiation, we should perform gain-of-function and loss-of-function studies in primary neurons. Better characterization of the function of JMY in different steps of neuronal differentiation will improve our understanding of the regulation of dynamic actin polymerization in neurons.